Chapter 5

Copper Orebody Geometry and Sulphide Assemblage

5.1 INTRODUCTION

The timing, origin and nature of copper mineralisation throughout the Zambian Copperbelt (ZCB) has been the subject of ongoing debate for the past 40 years, with previous studies proposing syngenetic, diagenetic and epigenetic models for the origin of the copper orebodies (e.g. Garlick, 1974; Annels, 1989; McGowan et al., 2003; Selley et al., 2005). Much of this difference in opinion stems from the fact that the ores are deformed and as a result primary ore textures have been modified or obscured.

In this study, the approach to resolving ore genesis at NKM has been to integrate observations made at a variety of scales. This methodology has been successfully employed by Gilligan and Marshall (1987) and Marshall et al. (2000) to discriminate between remobilised pre-tectonic mineralisation and syn-tectonic or post-tectonic phases of mineralisation. Key elements of deposit analysis include:

- examination of macroscale orebody geometry and grade distribution, and their relationships to stratigraphic and structural architecture; and
- meso-scale observations of sulphide and gangue phases that can be used to establish the degree of textural modification related to deformation.

Approximately 90% of the copper and cobalt sulphides are confined to one stratigraphic interval, that being the lower portion of the Copperbelt Orebody Member (COM) and the upper 5 to 10 m of the Mindola Clastic Formation (MCF). The sulphides occur as disseminations throughout the host lithology, preferentially aligned parallel to cleavage, along small structures cross cutting cleavage within a particular layer and within bedding parallel and cleavage parallel veins in high strain domains. The sulphide ores at NKM are relatively simple however the textural relationships are complicated deformation. This chapter aims to contribute to this ongoing debate by documenting the orebody geometry, broad grade distribution and sulphide assemblage at the NKM deposit and document any relationship within the sedimentological and structural frameworks developed in Chapters 3 and 4.

5.2 PREVIOUS WORK

Numerous unpublished company studies have documented different aspects of the sulphide assemblages at NKM (Internal Reports – ZCCM, archived at MCM, Kitwe Office). In general these reports provide good background information, however they were found to be of limited use as they lack the required rigorous geological context for the mineralogical descriptions, and could not be re-examined as they relate to parts

of the mine that are no longer accessible. Several published works provide more useful information. Jordaan (1961) documented the sulphide zoning across the NKM and focussed on the lateral and vertical zonation of sulphides detailing the main phases as pyrite-carrollite-chalcopyrite-bornite-chalcocite. Richards (1965) focused on describing the copper mineralisation geometry hosted in the basal portion of the MCF, herein termed the Basal Quartzite Orebody. As part of this his sedimentology study, Clemmey (1974) briefly described the vertical and lateral distribution of sulphides at Mindola North shaft and within the Mindola Pit (Fig. 5.1). Simmonds (1980) documented important sulphide phases and textures at the Baluba copper deposit and compared these results to a selection of samples from NKM concluding remobilisation of sulphide minerals at both deposits. In a more recent study focusing on veins and sulphides occurring within the Nkana Synclinorium Area, Brems (2009) suggest that the massive vein generation represents a separate mineralisation phase, not only resulting from local remobilization of sulphides, however concludes an overall multistage mineralising system of diagenetic and orogenic origin.

Several studies have documented and interpreted the orebody geometries, and sulphide assemblages and textures elsewhere in the Chambishi Basin and across the ZCB. Early works focussed on relationships between metal zonation and variations in facies architecture (Fig. 5.2), interpreting syngenetic sulphide precipitation at redox interfaces related to palaeo-shorelines (Garlick, 1961, 1972; Clemmey, 1974). Annels (1989) demonstrated that metal zonation/facies relationships are less systematic than previously described, and favoured a syn-diagenetic origin for the deposits. Based on regional scale alteration and the geometries of several ZCB deposits Selley et al. (2003; 2005) emphasised the systematic relationships between orebody shape, grade distribution, and structural/stratal architectures formed during early stages of basin development (Fig. 5.2). These studies concluded that the early basin configuration strongly influenced the passage of diagenetic ore-forming fluids, as well as redox architecture. Although these authors were uncertain of the absolute age(s) of mineralisation, they favoured multistage episodes that predated peak orogenesis. By contrast, McGowan (2003) documented evidence for a genetic link between orogenic structures and mineralisation at the Nchanga deposit, where the high grade parts of orebodies occur in close association with either layer-parallel shear zones or high angle structures that penetrate basement.

5.3 DATA SOURCES

Field data used to interpret the geometry of the main copper orebody was collected from several areas and sources. The majority of data were collected from the lower levels of SOB Shaft, within the Nkana Synclorium Area (NSA) where considerable recent drilling has occurred (Fig. 5.3). Twelve geological sections were constructed for the NSA as part of this study, as discussed in Chapter 4. The geometry of the copper orebody was assessed in relation to these geological sections and the 3360L geological plan. A basic three dimensional model using of the copper orebody was constructed from sections and drillholes within the NSA using Vulcan™ software. At Central Shaft, work was confined to the underground exposures and limited drilling from the Zero Syncline-Zero Anticline area (Fig. 5.3). Compilation of old mine plans and grade sections contributed to the work in this area. Historical mine data form the basis for analysis of a small satellite orebody, the Basal Quartzite Orebody, located near SOB Shaft (Fig. 5.3). Underground access to this particular area was restricted to the main access drives on the 1250L and 1530L which are parallel to the strike of strata, and thus of limited use. Compilation and interpretation of level plans and sections drawn for the Basal Quartzite Orebody at SOB Shaft have been used to ascertain the geometry of the copper mineralisation. At the Mindola and Mindola North shafts, the moderate- to steeply-dipping nature of the orebody allowed for vertical grade

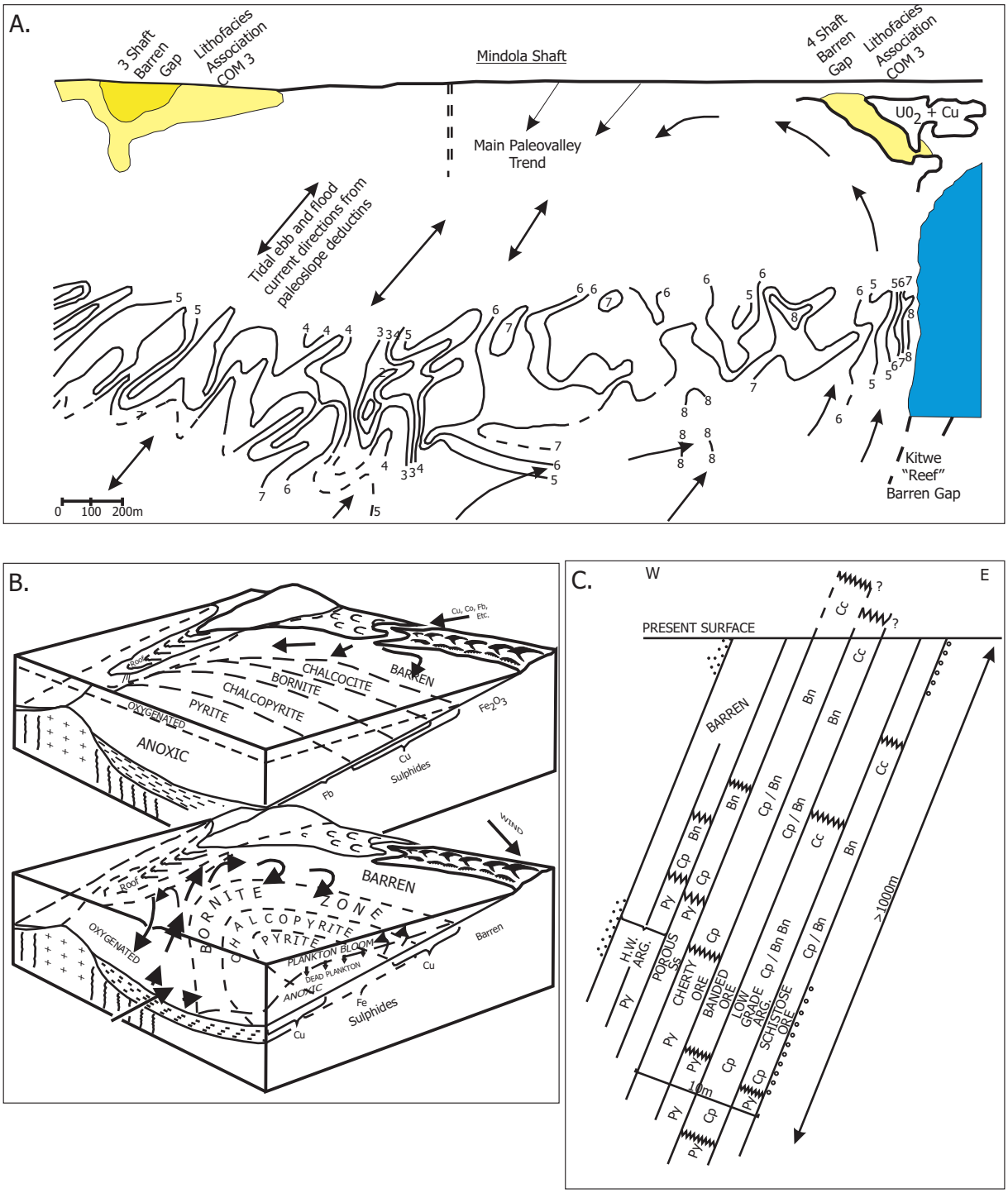

Figure 5.1. Longitudinal profile of the area between the Kitwe Barren Gap and the Mindola Shaft showing copper isogrades and postulated tidal current pattern (from Clemmey, 1974). Isogrades numbered 1 to 8 in order of decreasing grade. Clemmey postulated that the syngenetic copper grade distribution was controlled by tidal currents. b). Block diagrams showing diffusion of copper, cobalt, iron, and other metals in solution in an ocean environment – a syngenetic copper genetic model. The upper block diagram shows copper is only being precipitated in the near shore with increasing iron precipitation at depth which results in the sedimentary zoning of the minerals after diagenesis or metamorphism. The lower block diagrams shows the spatial distribution of metal and mineral zones anticipated with an upwelling current bringing metals from ocean depths. The upwelling would be induced by a longshore or offshore wind, forming sand dunes as observed along the eastern shore of the Mufulira 'C' orebody (from Garlick, 1984). c). The sulphide assemblage distribution relative to stratigraphy within the Mindola Pit during early stages of mining (from Clemmey, 1974). It was not possible to document the sulphide assemblage within the Mindola Pit during this study.

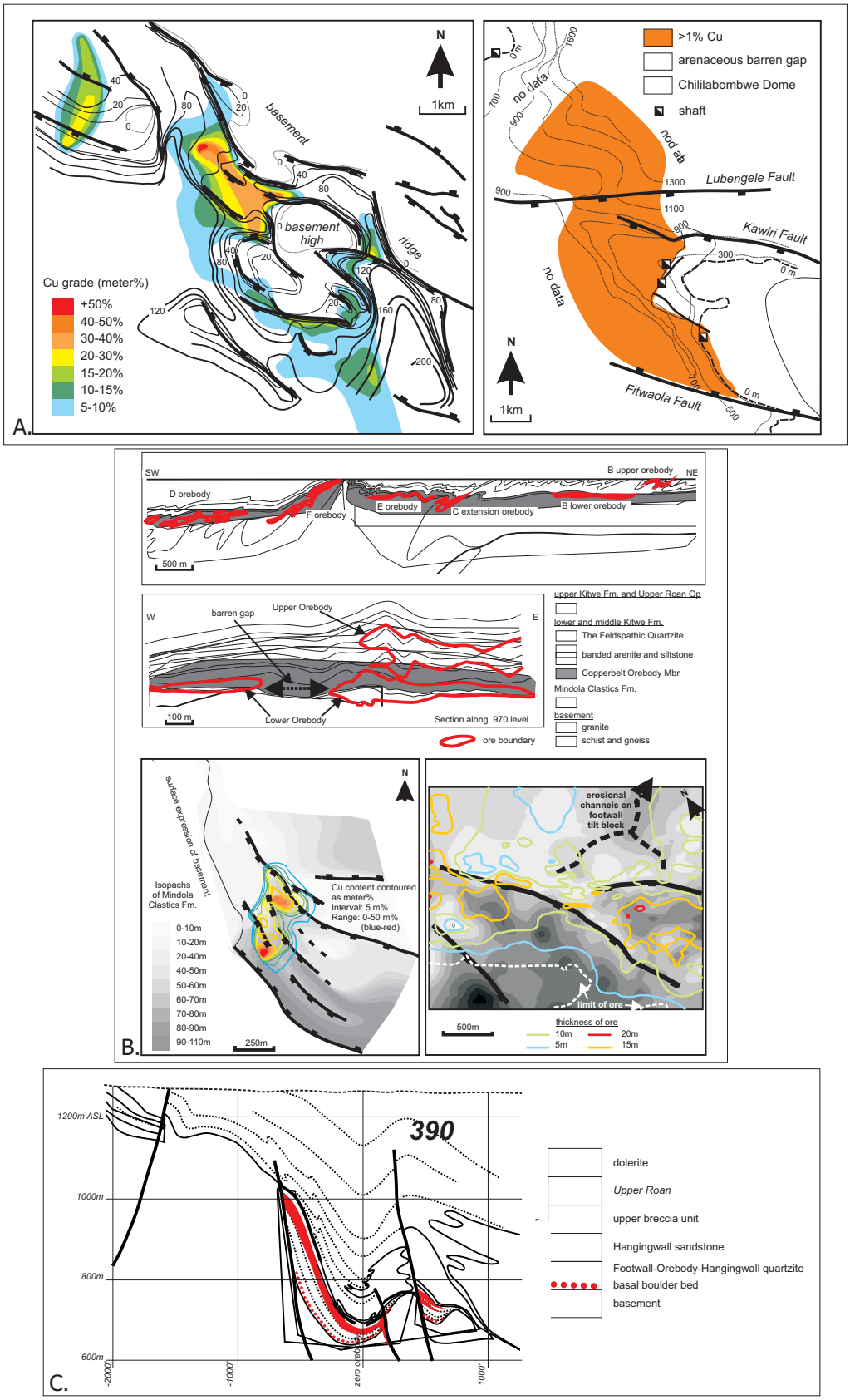

Figure 5.2. Examples of the distribution of copper mineralisation relative to interpreted basin structures and thickness changes in the MCF from weakly deformed deposits on the Zambian Copperbelt. a). The distribution of the copper mineralisation within the Ore Shale hosted deposits at Chambishi SE (left) and Konkola (right), demonstrate a relationship between grade and changes in the basin geometry (modified from Selley et al., 2005). b). Copper mineralisation hosted in the Ore Shale equivalent sequence at the Mufulira copper deposit was demonstrated to be coincident with changes in the basin structure (modified from Scott et al., 2003). c). Arenite hosted copper mineralisation closely related to basin structures at the Chibuluma B deposit (modified from Selley et al 2003).

profiles to be assessed from underground cross-cuts and drill core. Compilation and updating of current and historic mine longitudinal profiles and sections were used to ascertain the lateral distribution of the grade and where possible sulphide distribution from available drill core or historic logs.

5.4 RESOURCE OF NKANA-MINDOLA

The longevity of the mining operations at NKM has prevented an accurate determination of the global copper and cobalt resource. Kirkham (1989) and Hitzman et al. (2005) estimated a total resource in excess of 670 Mt @ 1.8% Cu and 0.10% Co, making the NKM deposit one of the larger copper deposits on the ZCB. The mine has produced in excess 5 Mt of copper since operations began in 1932. Underground exploration activities between 2000 and 2002 defined inferred reserves within Nkana Synclinorium Area at SOB Shaft of ~95Mt @ 2.3% Cu and 0.15% Co, with further ~90 Mt at 2.2% Cu and 0.14% Co in undeveloped reserves and resources across the whole deposit. The west limb of the Nkana Syncline hosts a currently uneconomic copper resource estimated at 91Mt @ 2% with an average true thickness of 2.3 m.

Oxidation of the primary sulphide orebody has taken place to a depth of at least ~100m, along the strike length of the NKM system. Several small pits exploit this resource and the oxidation zone passes down-dip into a mixed oxide-sulphide. The main copper minerals in the main oxide zone are malachite, chrysocolla, cuprite, tenorite, azurite and liberthenite. In the mixed oxide-sulphide zone the main minerals are bornite, chalcocite, covellite, carrollite, chalcopyrite, pyrite and native copper. Native copper and chalcocite (secondary) have been recorded at depths of ~800m in the far northern area of NKM (Jordaan, 1961). Understanding the secondary copper and cobalt phases, near-surface oxidation processes and the relationship to aquifers was beyond the scope of this study.

5.5 GEOMETRY, GRADE, AND SULPHIDE DISTRIBUTION IN THE COPPER-COBALT OREBODIES

The distribution of the main copper and cobalt mineralisation is confined to the immediate vicinity of the stratigraphic contact between the MCF and the overlying COM. Approximately 90% of the copper mineralisation at NKM is hosted within the dolomite-argillite and carbonaceous argillite facies associations (COM 1 and COM 2, respectively). The stratabound distribution of ore extends more or less continuously over a 15 km strike length along the north-eastern limb of the Nkana Syncline, as well as along the western limb. The copper orebody is defined as > 0.5% Cu, however the economic cut-off for mining purposes at NKM is generally defined as ca. > 1.2% Cu.

The combination of facies associations, in particular lateral variations at the level of the COM (chapter 3) and fold geometry configuration (Chapter 4), provide the framework within which to examine orebody geometry and sulphide distribution (Fig. 5.3). Two geometrically and compositionally distinct parts of the main orebody are recognised (Table 5.1). The northern part, defined as an area from ~3km south of the Kitwe Barren Gap along strike to the northwest to the edge of the Ichimpe Barren Gap, is predominately hosted by facies association COM 1 strata, and generally has a sulphide assemblage of bornite+chalcopyrite±pyrite (Figs 5.3 and 5.4). This area corresponds with the low- and moderate-strain structural domains (Fig. 5.3), incorporating the transition zone from a moderately westerly dipping orebody in the NW to a steeply dipping and open-folded orebody adjacent to Central Shaft. The southern part, centred around the SOB Shaft and extending around the hinge region of the Nkana Syncline to the west limb, is characterised by the facies

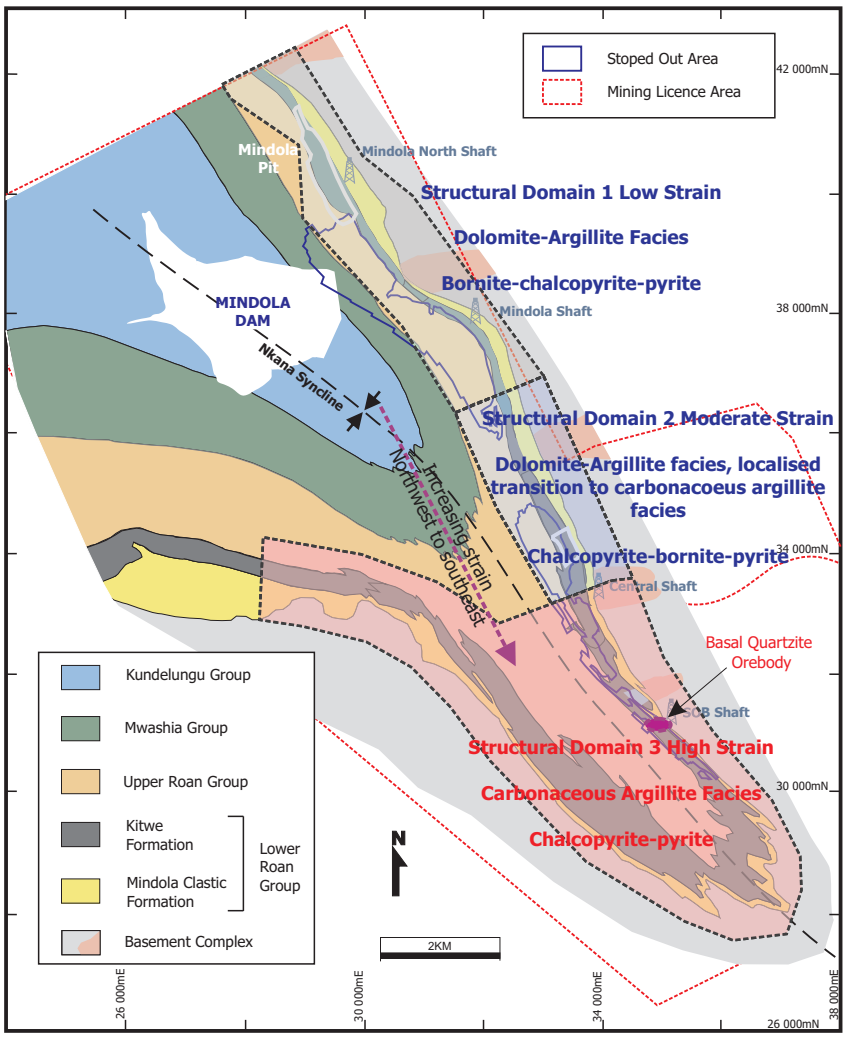

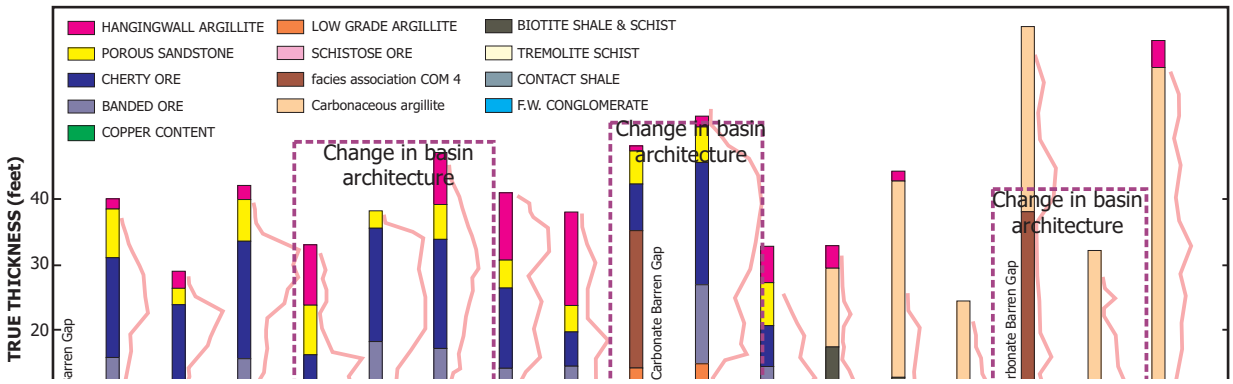

Figure 5.3. a). Surface geological map at NKM with the two key copper domains, based upon the facies association framework and the structural domains. The northern domain is marked in blue and the southern domain in red. There is an increase in strain at NKM from the northwest to the southeast. Mineralisation domain one has a dominant bornite-chalcopyrite-pyrite ore mineralogy and is hosted by dolomite-argillite facies associations (facies association COM 1). This domain incorporates the low and moderate strain structural domains previously described in Chapter 4. Mineralisation domain two has a dominant copper sulphide mineralogy of chalcopyrite-pyrite hosted by carbonaceous argillite-shale (facies association COM 2). This domain is coincident with the high strain structural domain. There is an overall a shift from a bornite-chalcopyrite dominant system in the northwest to a chalcopyrite-pyrite in the southeast, which is coincident with a shift from dolomite-argillite facies to carbonaceous argillite host lithology. There are local variations in the sulphide assemblages as well as vertical zonation of the sulphide minerals which will be discussed in this chapter. b). Lithology and grade distribution within the Copperbelt Orebody Member along the NE limb of the Nkana Syncline from the higher levels of the mining operations which have been mined out (modified from Jordaan, 1961).

associations COM 2 strata that host a chalcopyrite+pyrite dominated sulphide assemblage (Figs 5.3 and 5.4). Also included within this part of the system is the Basal Quartzite Orebody, an isolated arenite-hosted ore zone positioned within lower MCF rocks, comprising chalcopyrite and pyrite. Limited work was conducted along the western limb during this study due to the propensity of available historic drillcore. The copper grades are generally less than 1.2% copper on the west limb of the Nkana Syncline and have historically been defined as uneconomic due to the thin nature and steeply dipping geometry of the copper ore envelope.

The localised facies variations within the COM link to further partitions within the main orebody. Copper mineralisation (defined as >0.5% Cu) at the basal COM level of the stratigraphy is almost continuous for a strike length of ~15km along the NE limb of the Nkana Syncline, however, stratabound mineralisation is punctuated by barren or very low grade zones (< 0.2% Cu), known colloquially as 'barren gaps', that are coincident with changes to carbonate- or sandstone-facies associations at the base of the COM (facies associations COM 3 and COM 4, respectively (Figs 5.3 and 5.4). These changes in the facies of the COM have been documented as being related to the original syn-rift basin architecture (Chapter 3). Co mineralisation occurs throughout the copper orebody envelope at NKM, however is unevenly distributed. Uranium mineralisation is associated with certain arenaceous sandstone facies intervals (facies associations COM 3) (Jordaan, 1961).

Vertical sulphide zoning has long been recognised in certain Zambian copper deposits (e.g. Jordon, 1961; Annels, 1989; Sweeney and Binda, 1989). At NKM vertical (or more strictly, cross-stratal) sulphide zonation can be broadly identified across the MCF-COM boundary however this is not a consistent feature and needs to be considered with reference to the larger scale lateral zonation of the sulphides across the deposit (Fig. 5.4). Within the northern area, the vertical zonation is more pronounced and partially reflects the diverse lithotype hosting the sulphides, the differences in the copper and cobalt sulphide assemblages (i.e. bornite-chalcopyrite-pyrite-carrollite in the north compared to chalcopyrite-pyrite-carrollite assemblage in the south) and the relative low strain of the area.

5.5.1 Uranium Mineralisation

Volumetrically minor uranium mineralisation has been mined from an arenaceous facies variant of the COM (COM 3) along the southern flank of the number 4 shaft barren gap (Fig. 5.3a). Jordaan (1961) reported that in addition to lateral facies variation, the COM is half its normal thickness within the barren gap, with the lower argillaceous interval that hosts peripheral Cu-Co ore being largely 'replaced' by pebbly arkose or dolomitic sandstone. As argued in Chapter 3, arenaceous facies variants of the COM are considered to represent structurally-controlled sediment input points to dominantly argillaceous depocentres.

Uranium-bearing phases include uraninite, brannerite and coffinite (Jordaan, 1961; Notebaart andV ink, 1972). Darnley et al. (1960) reported as association of melonite ($NiTe_2$), and subordinate bornite, chalcopyrite, digenite, and chalcocite, with uraninite. Although minor Cu mineralisation is associated with uraninite, the U grade varies in an inverse ratio to Cu (Jordaan, 1961). A similar relationship, coupled with the presence of Ni-bearing phases, occurs in the uranium deposits of Congolese area of the Copperbelt (Jordaan, 1961).

5.5.2 Basement Mineralisation

No evidence of basement mineralisation was observed during this study. However, Jordaan (1961) reported disseminated sulphides, including chalcopyrite, bornite, carrollite, pyrite, molybendite and magnetite, in intensely micaeous altered basement quartzite and mineralised veins on the 2620L of SOB Shaft. Gangue mineral phases include muscovite, sericite, biotite, calcite, tremolite, actinolite, albite, scapolite and anhydrite.

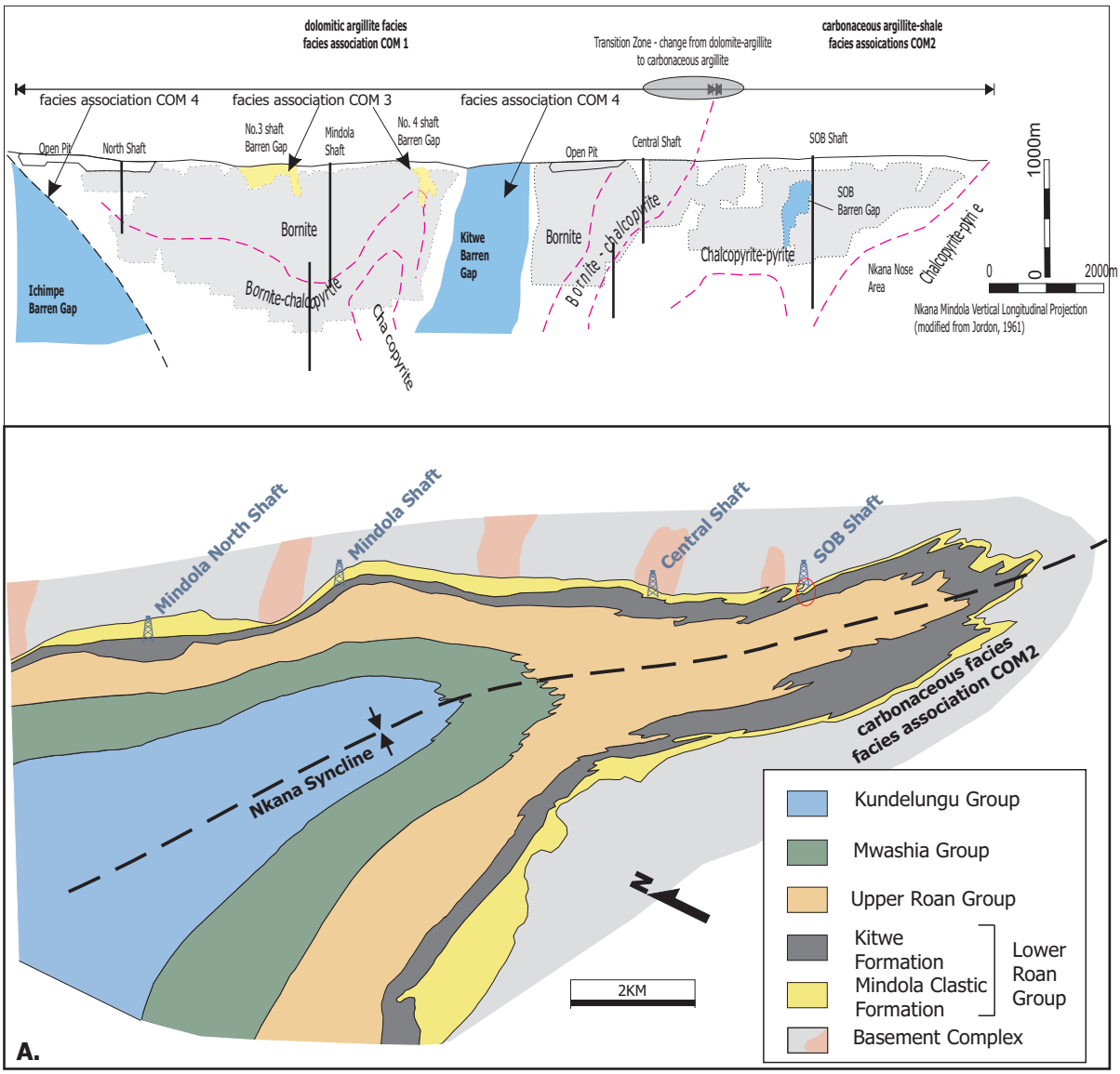
dolomitic argillite facies
facies association COM 1
Transition Zone - change from dolomite-argillite to carbonaceous argillite
carbonaceous argillite-shale
facies assoications COM2
facies association COM 4
facies association COM 3
facies association COM 4
Open Pit
North Shaft
No.3 shaft Barren Gap
Mindola Shaft
No. 4 shaft Barren Gap
Open Pit
Central Shaft
SOB Shaft
SOB Barren Gap
Bornite
Bornite-chalcopyrite
Cha-copyrite
Ichimpe Barren Gap
Kitwe Barren Gap
Bornite
Bornite - Chalcopyrite
Chalcopyrite-pyrite
Nkana Nose Area
Chalcopyrite-pyrite
1000m
0
0
2000m
Nkana Mindola Vertical Longitudinal Projection
(modified from Jordon, 1961)
Mindola North Shaft
Mindola Shaft
Central Shaft
SOB Shaft
carbonaceous facies
facies association COM2
Nkana Syncline
2KM
Kundelungu Group
Mwashia Group
Upper Roan Group
Kitwe Formation
Mindola Clastic Formation
Lower Roan Group
Basement Complex
A.

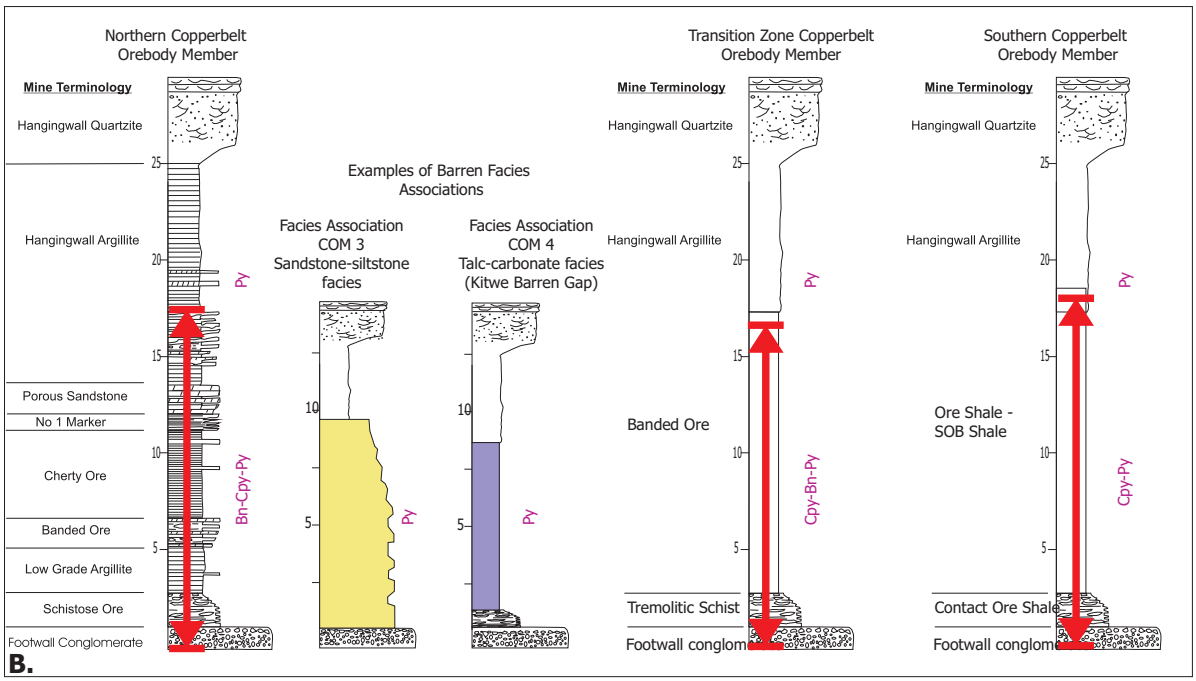
Northern Copperbelt
Orebody Member
Mine Terminology
Hangingwall Quartzite
Hangingwall Argillite
Porous Sandstone
No 1 Marker
Cherty Ore
Banded Ore
Low Grade Argillite
Schistose Ore
Footwall Conglomerate
Py
Bn-Cpy-Py
Examples of Barren Facies Associations
Facies Association COM 3
Sandstone-siltstone facies
Facies Association COM 4
Talc-carbonate facies
(Kitwe Barren Gap)
Transition Zone Copperbelt
Orebody Member
Banded Ore
Tremolitic Schist
Footwall conglom
Cpy-Bn-Py
Southern Copperbelt
Orebody Member
Ore Shale -
SOB Shale
Contact Ore Shale
Footwall conglom
Cpy-Py
B.

Table 5.1. Summary of the characteristics of the copper orebody at the Nkana-Mindola Deposit.

Northern Mineralisation Part – Dolomite-argillite; Low to moderate strain structural domain	
Stratiform sulphide distribution	Location
	Mindola Shaft area – dolomite argillite host, locally transgresses to upper portion of MCF.
Concentration of sulphide in coarser grained, silty bands	
Concentration of coarser grained sulphides along bedding planes.	
Sulphides may occur as clusters/aggregates parallel to bedding and inter-grown with quartz, phlogopite and microcline.	
Bedding sub-concordant small veins with sulphides, pinching and swelling, recrystallization common and alignment parallel to cleavage.	
Carbonate-quartz-anhydrite nodules and disseminated pyrite	Upper portion of the COM, particularly hangingwall argillite unit
Southern Mineralisation Part – Carbonaceous argillite; high strain structural domain	
Stratiform sulphide distribution	Location
Disseminated elongate blebs, aligned parallel to cleavage	SOB to Central Shafts; key area Nkana Synclinorium Area.
Concentration of sulphide on mesoscale in small fold hinges.	
Sulphide disseminated in cleavage parallel veins; sulphide recrystallised.	
Coarse masses of recrystallised sulphide with irregular form near the base of the COM.	
Chalcopyrite aggregates immediately adjacent to D3 fault zone.	
Strain shadows forming around only cubic pyrite grains	
All veins have the same sulphide mineralogy as the adjacent argillite	
Mineralised veins only occur within the gross boundaries of the copper orebody; upper portion of the MCF or the lower COM.	
Carbonate-quartz-anhydrite nodules and disseminated pyrite	Upper portion of the COM, particularly hangingwall argillite unit

Table 5.2. Summary characteristics of the main sulphides occurring at NKM.

Texture	Mineralogy / Alteration	Key Attributes
Disseminated rounded to sub rounded grains	Pyrite	Small rounded grains, no visible alignment to deformation fabrics
Euhedral Grains	Pyrite Carrollite	Variable deformation – simple or complex fractures with retention of the grain shape and also localized dispersion of fragments. Some grains have associated pressure shadows parallel to foliation Fractured pyrite grains infilled by chalcopyrite, pyrrhotite. Pyrite and carrollite grains enclosed by chalcopyrite.
Cleavage Parallel Sulphides	Chalcopyrite Bornite Pyrrhotite Pyrite Phlogopite Quartz Sericite	Planar S_3 parallel chalcopyrite-bornite Terminated by vein related sulphides and massive quartz blows with sulphides Folded chalcopyrite aggregates. Late D_4 shears cross-cut the foliation and copper sulphides can be remobilised adjacent to the structure.
Massive sulphide	Chalcopyrite Bornite Pyrrhotite Pyrite Carrollite Quartz Calcite-Dolomite Phlogopite	Massive blows and breccia matrix in deformed host rocks. Mixed sulphide assemblage Cross-cut S_0 and S_3 Occur near the boundary between of the MCF-COM. No alteration associated with blows. No evidence of aligned textures.

OPPOSITE: Figure 5.4. a). Plane of ore projection for the sulphide distribution at Nkana-Mindola, compiled from MCM data, Jordaan (1961) and Garlick (1989) incorporated with a district scale map of the Nkana-Mindola deposit, showing broad down-dip and lateral (southward) sulphide mineral zonation from bornite (bn), to bornite and chalcopyrite (cpy), to chalcopyrite and pyrite (py). Orebodies are separated by arenaceous and dolomitic barren gaps. The dolomitic argillite facies of the Copperbelt Orebody Member occurs only in the region of sediment input points (arenaceous barren gaps). The Basal Quartzite Orebody is located on the southern side of SOB Shaft (noted by a red circle) and the rectangle box near the SOB Shaft defines the Nkana Synclinorium Project Area. Section – Orebody geometry and sulphide distribution. The northern domain is dominated by bornite-chalcopyrite and the southern domain is characterised by chalcopyrite-pyrite. The west limb of the Nkana Syncline is within the chalcopyrite-pyrite southern domain. b). Mine terminology subdivision of the COM. Vertical zonation within the orebody is recognised however is variable across the area. A hangingwall pyritic halo is always associated with the orebody.

5.5.3 Northern Part of the COM orebody

Lateral Variations

This section progressively examines the northern part of the main orebody from north to south. The northern-most area is accessed via two shafts, Mindola and Mindola North Shafts. The copper orebody at Mindola North Shaft extends for ~3km south from the Ichimpe Barren Gap and includes the historical Mindola Open Pit resource (Figs 5.4 and 5.5) It is 5 to 12 m thick, macroscopically parallel to the moderately WNW dipping stratigraphy, and confined to the basal portion of the COM. However, in detail the orebody envelope is transgressive of stratigraphy, with the assay-footwall and -hangingwall contacts not confined to a specific stratigraphic boundary.

Lateral and down-dip variations in the Cu-grade and sulphide assemblages at the Mindola North Shaft orebody are shown in Figures 5.5a and 5.5b. The effects of supergene enrichment within the near surface environment are evident in Figure 5b. Below this zone is a central domain of relatively low grade mineralisation that ranges from ~1.5% Cu to <1% Cu with increasing depth, however, is flanked by relatively high grade domains. The northern high grade domain coincides with the margin of the Ichimpe Barren Gap (Fig. 5.5a), along which there is abrupt thinning of the MCF and a corresponding inflexion in the strike of the MCF-basement contact (Fig. 5.6). Stratal/structural relationships with the southern high grade domain in the region of North Shaft remain unconstrained due to lack of historical data and present underground access. Variations in Cu grade appear broadly consistent with variations in sulphide composition documented in historical drillhole logs, which indicate bornite>chalcopyrite in higher grade domains, chalcopyrite>bornite in lower grade domains (Fig. 5.5b), and chalcopyrite-pyrite at deepest levels (Fig. 5.5a). Consistent higher copper grades are more continuous towards the southern edge of the North Shaft orebody, however this was not accessible underground at the time of the study.

In the Mindola Shaft area, comprehensive grade distribution data are only available on deep levels, where the broadly 8 m thick stratabound orebody dips steeply southwest. Copper grades at these levels are generally high throughout (Fig. 5.5a). Anomalously elevated Cu grades (>3.5%) occur in the immediate vicinity of the shaft, at an interpreted transfer zone and on the northern side of the Kitwe Barren Gap (Figs 5.4a and 5.5a). As is the case with the flank of the Ichimpe Barren Gap to the north, the increased grade in the immediate vicinity of the Mindola Shaft is coincident with a rapid thinning of the MCF and a change in the geometry of the basement-MCF contact. Furthermore two small arenaceous barren gaps (facies association COM 3) have been identified on the upper levels of the mine at Mindola Shaft adjacent to these localities (Jordaan, 1961). Along the northern flank of the Kitwe Barren Gap, bornite persists as the dominant sulphide at depth (Fig. 5.5a) (Jordaan, 1961; Garlick, 1972*)*.

On the immediate southern flank of the Kitwe Barren Gap, within an area of moderate strain and transition between COM 1 and COM 2 the copper isograde profile indicates relatively low values (Fig. 5.7b). A similarly positioned, yet more extensive zone of low grade Co values is shown in Fig. 5.7c. Although insufficient data exist to examine detailed sulphide zonation patterns, the obtainable information indicate chalcopyrite>bornite dominated assemblages in the low grade zone, passing southward into bornite dominated assemblages (Fig. 5.7a). The transition from the northern part to the southern part is coincident with a subtle change in the overall strike of the basement-MCF contact to the north of Central Shaft. There is also an apparent NW plunge to the high grade zone.

Vertical Variations

The vertical sulphide and grade distribution is best considered within the context of lithological variations throughout the profile of facies association COM 1(dolomite-argillite facies). For this purpose, local mine stratigraphic nomenclature is used. In the northern-most area (i.e. North Shaft and Mindola Shaft) this involves, from base to top, the Footwall Sandstones, Schistose Ore, Low Grade Argillite, Banded Ore, Cherty Ore and Porous Sandstone units (Fig. 5.8). Appendix one contains detailed descriptions of each of these mine units. The profiles shown in Fig. 5.8 were logged and analysed as part of this study. Although vertical sulphide and grade zoning is evident in each profile, there is little obvious consistency in detail, and profiles are too widely spaced to resolve what are likely complex, localised relationships between mineralisation and lithostratigraphy. However, some important generalisations may be made. The lower portion of the COM at Mindola Shaft is low grade with higher copper grade present in the Banded and Cherty Ore units (Fig 5.8). Chalcopyrite and bornite are disseminated throughout each of these units. Carrollite is typically confined to middle units including Banded Ore, Chery Ore, No.1 Marker and the Porous Sandstone units. Minor enrichment in Co is sometimes located at the hangingwall assay boundary and appears to be associated with increasing portion of pyrite and not carrollite. Pyrite is predominantly only found in the assay hangingwall, outside the copper orebodies (>1.2% Cu) and may sometimes be associated with elevated values of Co in range of 0.1 to 0.15% Co.

5.5.4 Southern Part of the COM orebody

Lateral Variations

The southern part of the COM orebody is within the high strain structural domain and hosted by carbonaceous-carbonate argillite of facies association COM 2 (Fig. 5.3). The transition between the northern dolomite-argillite lithotype of the COM and the carbonaceous-carbonate argillite of the southern domain occurs on the southern side of Central Shaft and is coincident with an overall shift from a WNW striking geometry of the MCF-basement further to the south to a dominant NW striking geometry to the north. The broadly stratabound copper ore envelope conforms to the geometry of the complexly folded MCF-COM interface (Figs 5.9 and 5.10) The copper orebody is primarily hosted in the basal portion of the COM, but locally extends down-section into the upper MCF within fold hinges, where concomitant structural thickening of the COM and broadening of the ore envelope also occurs (Figs 5.9 and 5.11). Chalcopyrite, carrollite, pyrite and minor vein hosted bornite are hosted within this interval. The contact between the orebody and assay hangingwall is transitional does not correspond to a lithological change in the COM and is recognised by an increase in pyrite at the expense of chalcopyrite. In fold limbs, the average thickness of the copper orebody is ~5-10 m, however a sub-economic zone (i.e. <0.5% Cu) commonly extends 3-5m stratigraphically above the assay hangingwall. By contrast, the orebody may exceed 50m in thickness within major fold closures (Fig. 5.9). Localised D_4 shear zones within the argillite units further complicate the copper orebody geometry on the mesoscale. Cobalt mineralisation only occurs within the copper orebody envelope and the cobalt distribution in the higher strain domains increases around fold hinges, along portions of the fold limbs (west limb of 'C' anticline) and in the upper portion of MCF within the NSA at SOB Shaft.

Sufficient data were available to examine Cu grade distribution about folded surfaces within the NSA. Overall the copper grade in the southern part is lower than in the northern part mainly due to a change in the copper species to chalcopyrite + pyrite in the southern part. Within the NSA, the highest grade of copper coincides with the hinge of the 'C' anticline and ca. 20% of the mineralisation in the fold hinge is hosted within the upper portions of the MCF (Figs 5.9, 5.13 and 5.14). The copper orebody is continuous although thin on the limbs of the 'C' syncline and 'C-D' anticline-syncline, while is particularly thick around the 'C' anticline (Fig.

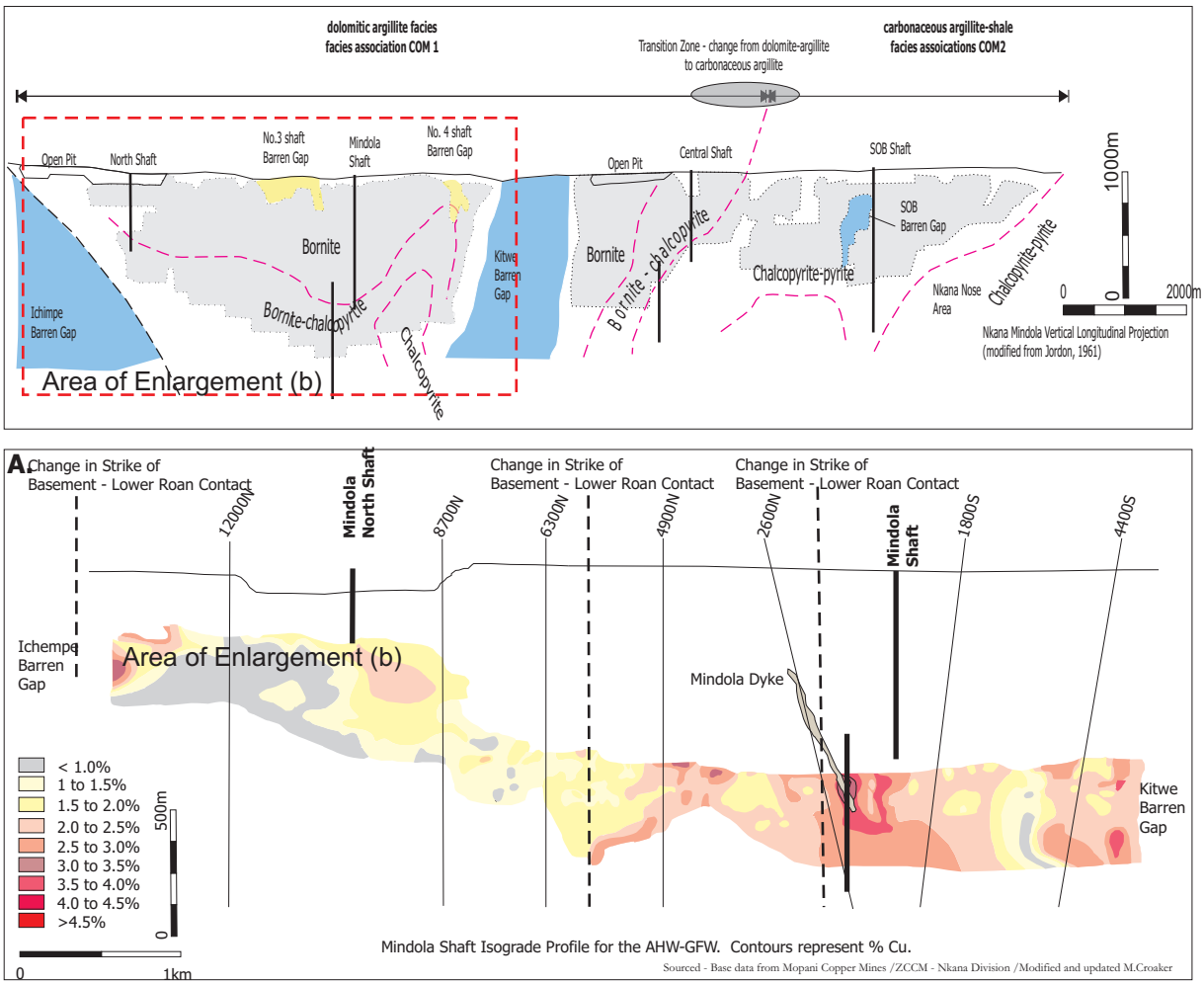

Figure 5.5. Grade and sulphide distribution profiles for the Mindola North Shaft and Mindola Shaft areas within the northern domain. Apart from the increase in grade associated with supergene processes, there is an increase in grade associated with the northern flanks of the Kitwe Barren Gap (5a), related to the central area of Mindola Shaft which is coincident with a change in the geometry of the basement-MCF contact and adjacent to the southern flank of the Ichimpe Barren Gap (5b). Figure 5b is a rotated to horizontal plan.

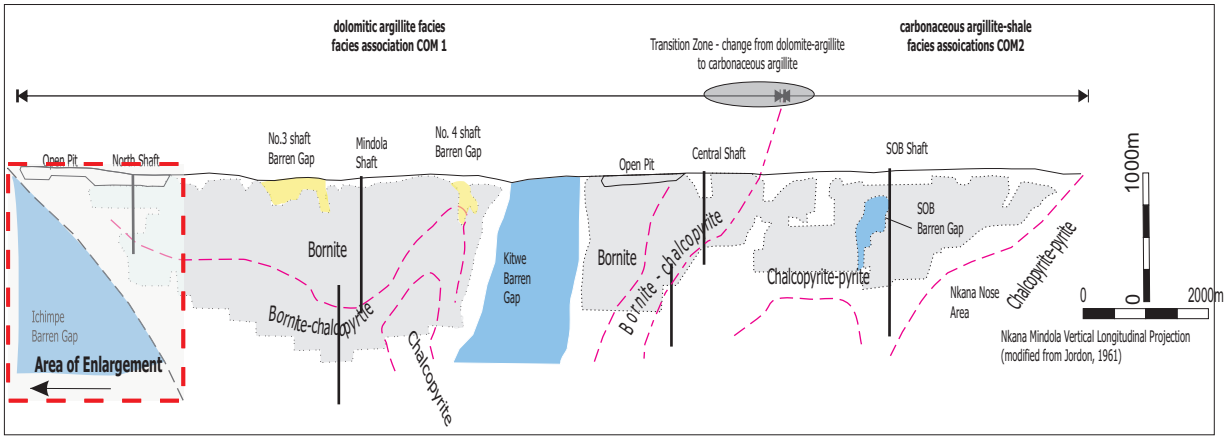

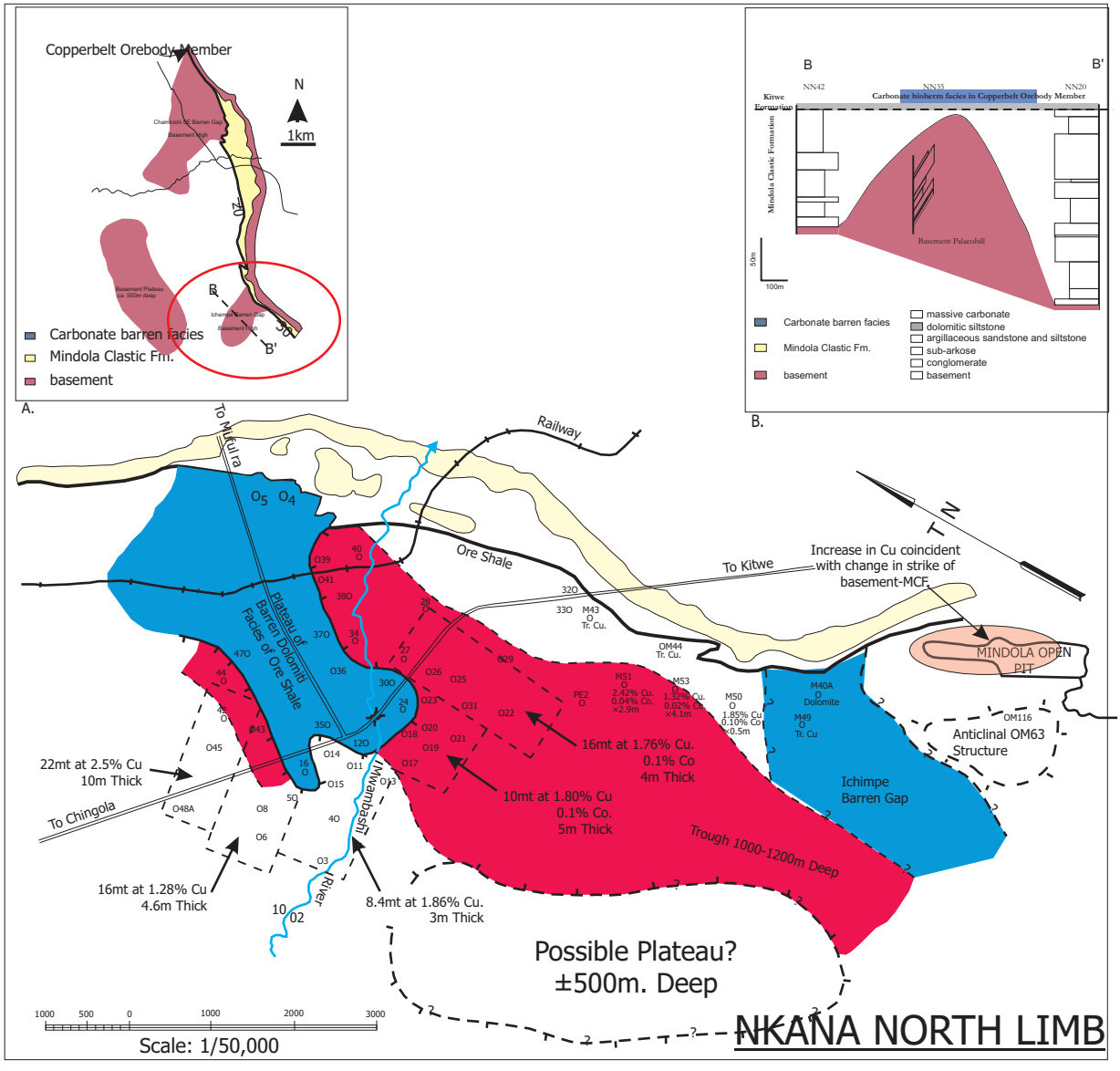

Figure 5.6. Plan map of the Mindola North Shaft, Ichimpe Barren Gap and the southern flanks of the Chambishi SE prospect area demonstrating the lack of mineralisation associated with the Ichimpe Barren Gap (facies association COM 4) and the change in the geometry of the basement-MCF contact which is coincident with the Ichimpe Barren Gap (modified from ZCCM plan (1974) held by Mopani Copper Mines). The distribution of copper mineralisation was documented by Selley et al. (2005) for the Chambishi SE Prospect as shown in Figure 5.2a.

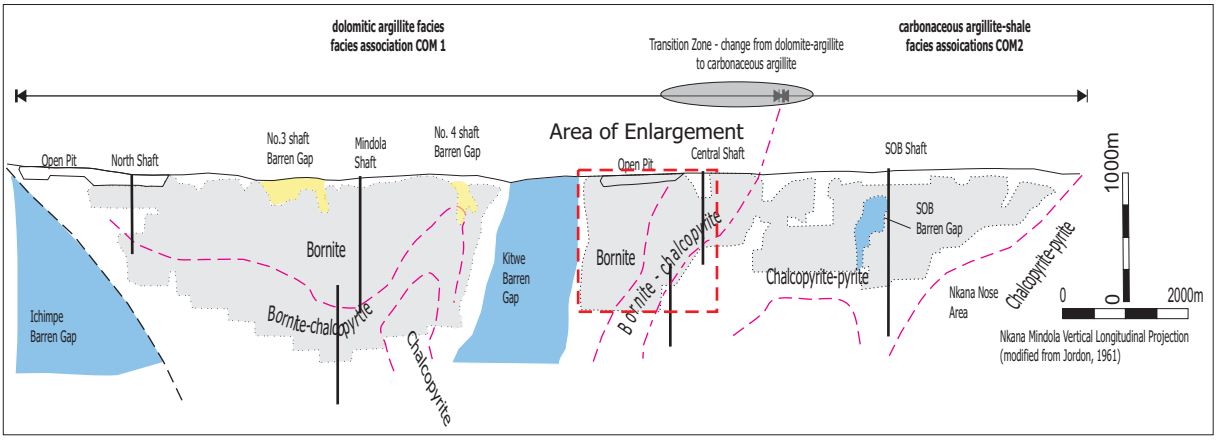

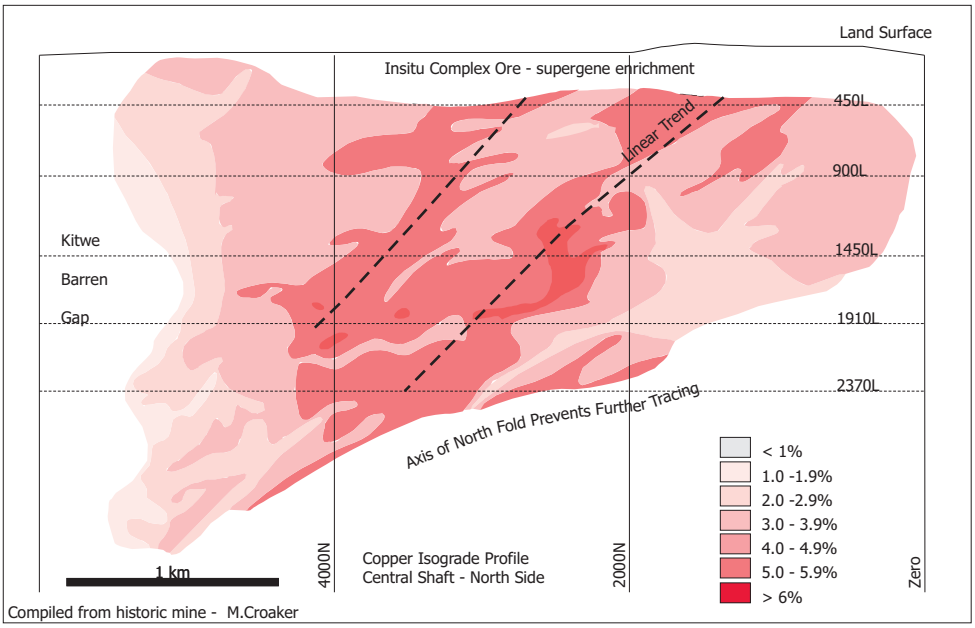

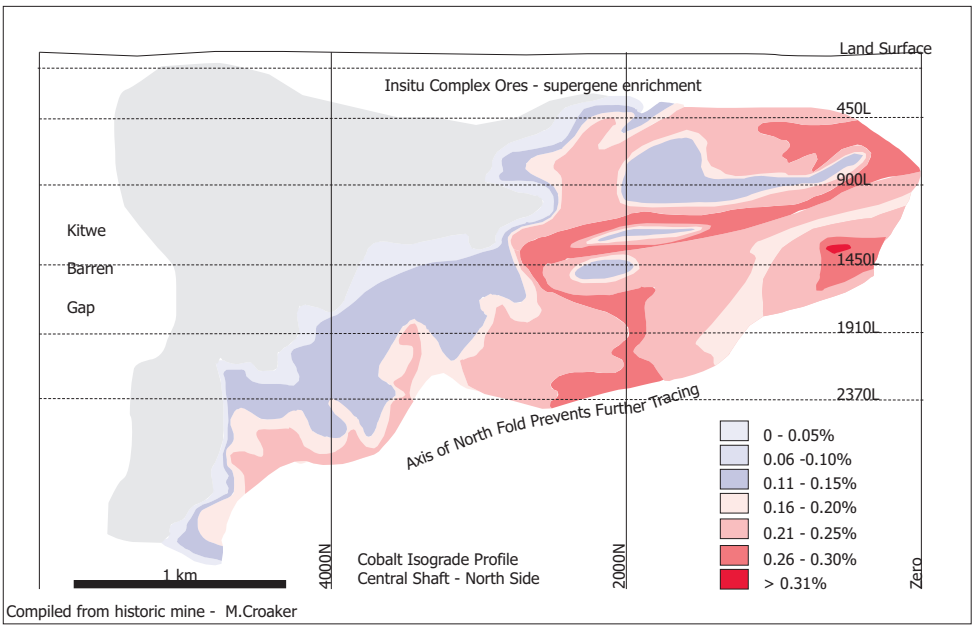

Figure 5.7. Grade distribution of copper and cobalt, immediately to the south of the Kitwe Barren Gap, hosted within dolomitic-argillite to carbonaceous argillite rock on the moderate to steeply northeast limb of the Nkana Syncline. Bornite-chalcopyrite-pyrite is the sulphide assemblage within this area. There is a larger zone of lower cobalt compared to copper on the southern flank of the Kitwe Barren Gap.

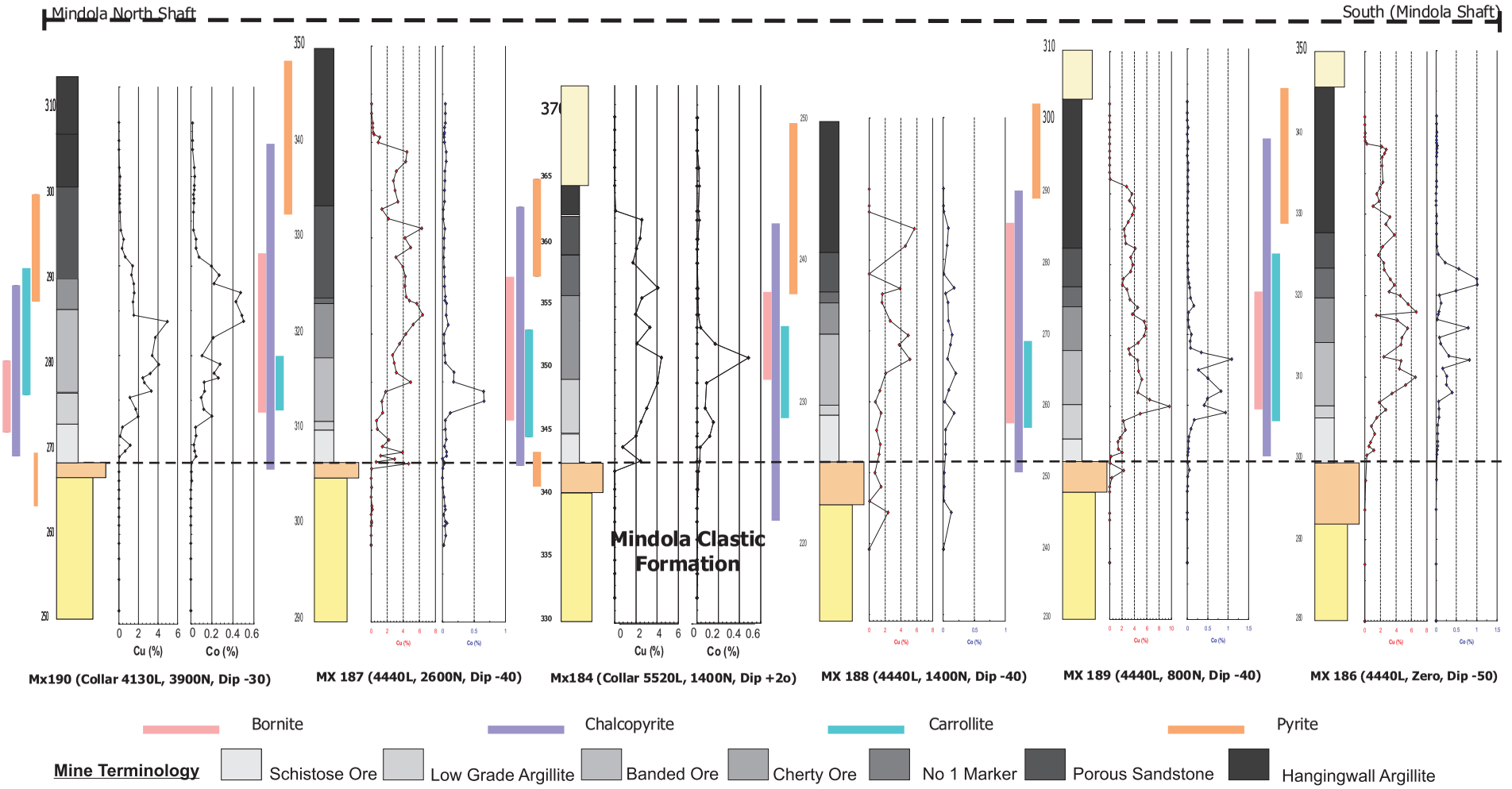

Figure 5.8. Vertical zonation of grade and sulphide assemblage in the northern domain, hosted by facies association COM 1, dolomite-argillite rock. The Banded Ore and Cherty Ore units commonly have higher grade material and a bornite dominant sulphide assemblage. Pyrite is disseminated throughout the immediate hangingwall rocks to the orebody. Cobalt, mainly in the form of carrollite, is commonly concentrated in the Banded Ore unit.

5.9). This is coincident with rapid changes in the thickness of the MCF and was described being related to a basin transfer zone (Chapters 3 and 4).

The three dimensional geometry of the cobalt ore envelope was unable to be mapped due to the inconsistent distribution of the cobalt mineralisation. The higher cobalt values are commonly concentrated in the immediate vicinity of the MCF-COM contact and along the margins of the ca. 1.0% Cu assay cut-off boundary (Digital Appendices 3-6). Significant enriched in cobalt is associated with the upper flanks and crest of the 'C' anticline, within the overall copper orebody (Digital Appendices 3 and 4). Within the NSA, the tremolite-dolomite-calcite-k-feldspar rich upper portion of the MCF and lower Contact Ore Shale unit (mine terminology) commonly has higher values of cobalt compared to the COM, however these cobalt rich intervals are still within the bounds of the copper orebody (Fig. 5.16)

Importantly, despite the structural complexity of area, which affects the local vertical and lateral distribution of Cu mineralisation, the folded copper orebody has a stratbound geometry.

5.5.5 Basal Quartzite Orebody

A small arenite-hosted (MCF) copper orebody is positioned immediately adjacent to the SOB Shaft. Although arenite-hosted ores form important resources in many ZCB deposits, this orebody is an anomaly at NKM, being isolated from the main COM-hosted ore zones, consistently low in Co grade, and comprising less than 10% of the global resource. It was mined out in the 1960's and remains inaccessible today, however sufficient historical data exist to recognise systematic links to early-formed basin architecture.

Level plans and sections show the orebody is hosted in a small synclinal structure in the Basal Quartzite Member of the MCF, just above the contact with the basement complex (Fig. 5.17). The lower MCF is thickest within the core of the syncline, becoming thinner on the eastern limb, and absent on the faulted out western limb (Figs 5.17b and 5.17c). This stratal geometry is consistent with a fault-controlled sub-basin depositional configuration, as shown in unrolled sections (Figs 5.17d and 5.17e). Based on the schematic sections and unrolled sections there is an interpreted 'basement high' positioned at the north-western edge of the sub-basin which appears to have remained a relative positive topographic feature during COM sedimentation, as indicated by a coincident lateral facies change from carbonaceous argillite (COM 2) to dolomitic facies (COM 4) (Fig. 5.17).

The orebody has a broadly coincident geological and assay hangingwall, the former corresponding to the boundary of the medium-grained quartz-feldspar-dolomite sandstone of the Basal Quartzite and conglomeratic unit of Kafue Arenite member (Figs 5.17c and 5.17d). There is no obvious geological footwall, the lower assay boundary locally transgressing strata of the Basal Quartzite Member to deeper stratigraphic levels along the eastern flank of an interpreted inverted basement-cored horst (Fig. 5.17d). Thus, the orebody is not strictly stratabound, and further contrasts with the stratal geometry of the COM-hosted ores (notably absent in this region) in that it has limited strike length. The orebody is restricted to the most condensed, southern portion of the MCF sub-basin, terminating over a strike length of ~200m with progressive north-westerly thickening of the MCF (Fig. 5.17). The distinctive geometric features of the orebody, its limited strike length, restriction to an along axis termination of an arenaceous sub-basin, pronounced geological hangingwall, yet indistinct geological footwall, are all typical of other ZCB arenite-hosted ores (Selley et al., 2005).

5.6 MESOSCOPIC TEXTURAL VARIATION IN THE MAIN CU-CO OREBODY

5.6.1 Northern Part

Sulphides are meso- and microscopically distributed in several different forms that vary in accordance with host lithotype, the gross geometry of the Cu orebody and the intensity of strain. Within northern domain the sulphides occur as stratiform disseminations with an apparent association of coarser grained sulphide within more silty horizons (Fig. 5.18a). These coarser grained layers have been recrystallised during metamorphism and the dominate mineralogy in varying proportions is dolomite, albite, quartz and phlogopite (Figs 5.18b and 5.18c). Bornite and chalcopyrite occur as medium to coarse grained blebs and intergrown aggregates. With increasing strain on the lower levels at Mindola Shaft, the sulphides are disseminated along bedding horizons, aligned parallel to cleavage, within small gashes-fractures and hosted in bedding parallel veins (Figs 5.18d and 5.19a-c). Within the upper portions of the ore sequence, intervals containing elongated nodules of carbonate, anhydrite, quartz and sulphides occur which are very similar to those observed in the southern domain (Figs 5.19e and 5.19f). The nodules range from 0.5 to 3 cm in length and mainly contain pyrite, however chalcopyrite may occur rimming the nodules.

5.6.2 Southern Part

The carbonaceous argillite at SOB Shaft and along the western limb of the Nkana Syncline host chalcopyrite, pyrite, carrollite and minor bornite typically aligned parallel to S_3 and confined to the lower portion of the COM, however mineralisation does occur in the upper portions of the MCF. The ore minerals also occur in several vein generations parallel to bedding, S_3 fabric and cross cutting S_3 fabric (Fig. 5.20). Copper mineralisation does occur in the basal zone of the COM in the Contact Ore Shale (COS - mine terminology) (Fig. 5.21). This basal alteration zone of the COM has similar mineralogical and textural characteristics to the Schistose Ore at Mindola, however contains a higher proportion of dolomite, phlogopite and tremolite. The unit has disseminated bornite, carrollite and chalcopyrite typically aligned parallel to S_3 within this folded sequence. The Contact Ore Shale may contain a higher proportion of carbonate mineral gangue phases than the immediately overlying carbonaceous argillite.

In hand specimens tight to isoclinal folding of the carbonaceous argillite commonly results in fold hinges containing cores of coarse-grained chalcopyrite ± pyrite-carrollite-bornite (Figs 5.21a-d). In thin section, the coarse-grained chalcopyrite ± pyrite-carrollite-bornite is accompanied by calcite-quartz-dolomite-phlogopite. The phlogopite is typically aligned axial planar to the F_3 folds and parallel to the main F_3 foliation. Localised concentrations of chalcopyrite, calcite, phlogopite and pyrite form in the hinges of F_3 folds and small scale D_4 fault propagation folds. All chalcopyrite and bornite hosted within the MCF typically occur as disseminated aggregates ranging in size from 0.5 mm to greater than 2-3 mm in size.

Meso-scale isoclinal folding of carbonaceous beds is common. Fractures in the hinges of the folded rocks are normally very fine (<0.1 mm wide) and can be infilled by quartz-calcite as well as chaclcopyrite ± pyrite. Coarse-grained chalcopyrite is common within the fold hinges. Mesoscale local deci-centimetre scale brecciation-fracturing of the more competent intervals of the carbonaceous dolomitic argillite does occur, with infilling generally in the form of calcite-quartz and chalcopyrite and more rarely, bornite (Fig. 5.22). Brecciation is typically restricted to the hinge zones of 3rd order folds. Within veins, there is no preferential elongation of the chalcopyrite and all sulphide hosting veins are restricted to the bounds of the copper orebody envelope and the sulphide phase hosted in the vein is commonly the same as the host rock sulphide phase. Many of these syn-tectonic veins contain more than one fibre layer, suggesting that deformation and mineral precipitation

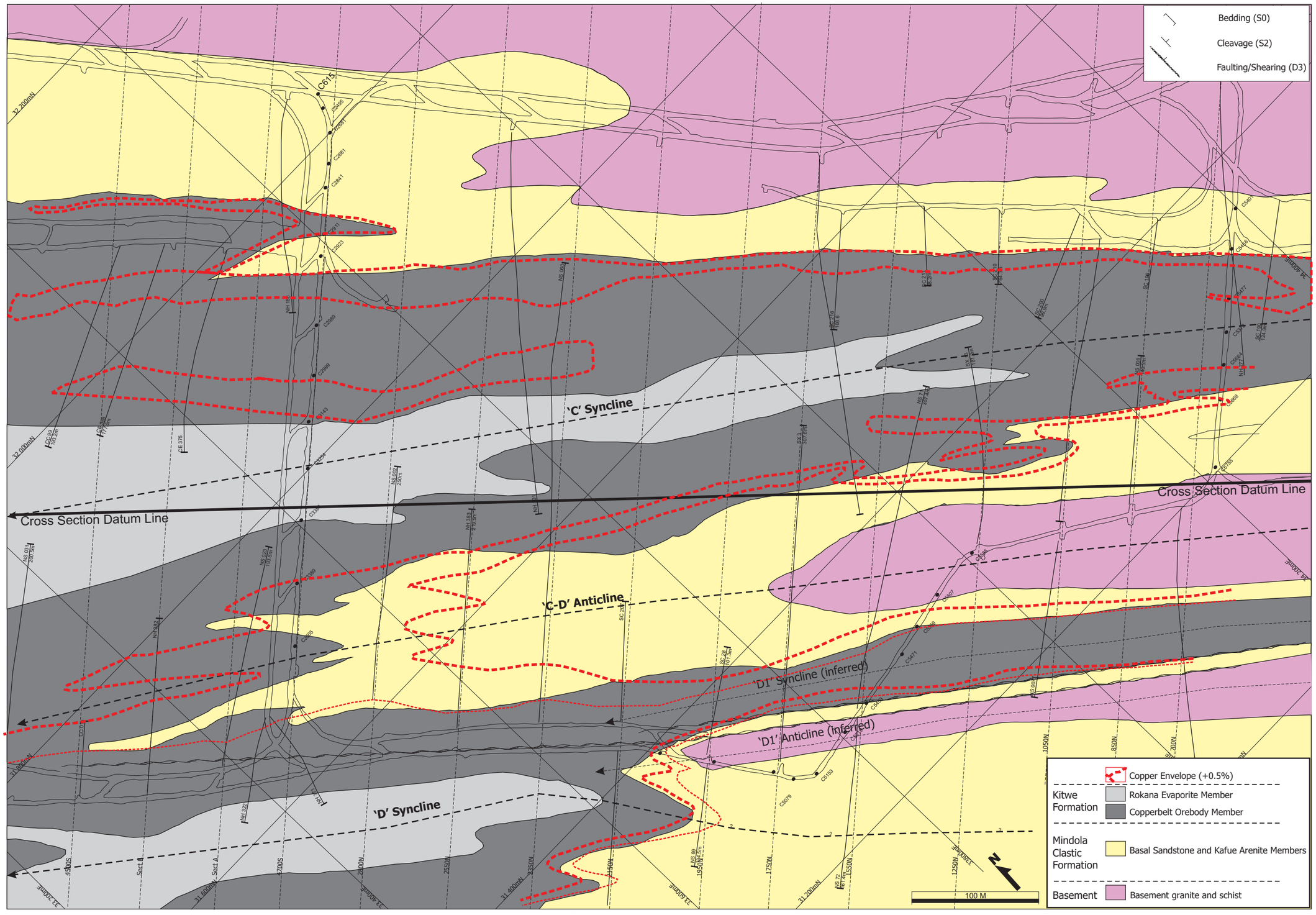

Figure 5.9. Simplified geological plan of the 3360L at SOB Shaft, constructed from underground mapping and logging of drillholes. The outline of the copper envelope (>0.5% Cu) shown in red. The northwest plunging 'C' syncline and anticline are the dominant 2nd order F3 folds identified at this location. This area is within the high strain structural domain at NKM. A copy of the original scanned hand drawn geological plan map and cross sections are located in digitial appendix 3. The copper ore envelope is depicted as a thicker line in these examples.

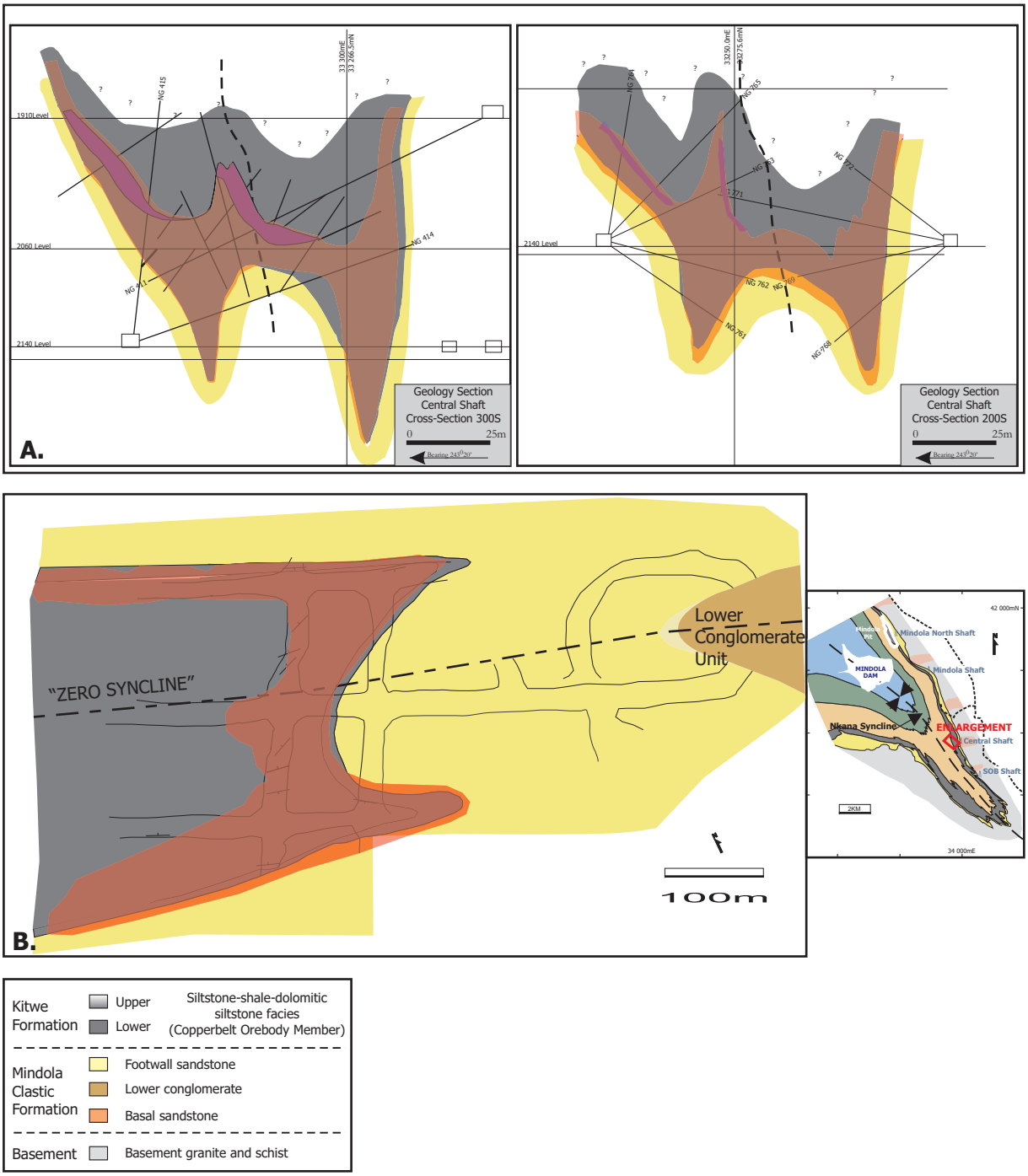

Figure 5.10. a) Geological sections of the broad Zero Syncline at Central Shaft depicting the broader open F2 folding within the moderate strain structural domain. The copper ore envelope (>0.5% Cu) is depicted in red and exhibits a folded geometry. High grade cobalt (>0.2% Co) shaded in blue. Section constructed from underground mapping and interpretation of drillholes. b). Geological plan map of the Zero Syncline (2320 L). The Cu ore envelope is clearly folded and transgresses the MCF-COM stratigraphic contact. The plan map is located about 500m north of the sections, due to access restrictions on the 2140L 200 to 300S cross cuts.

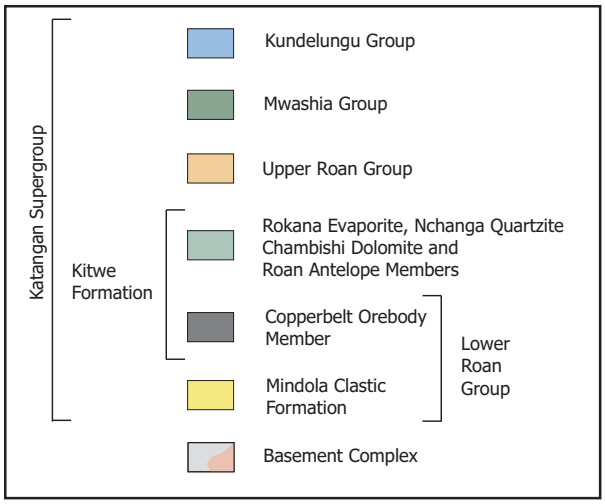

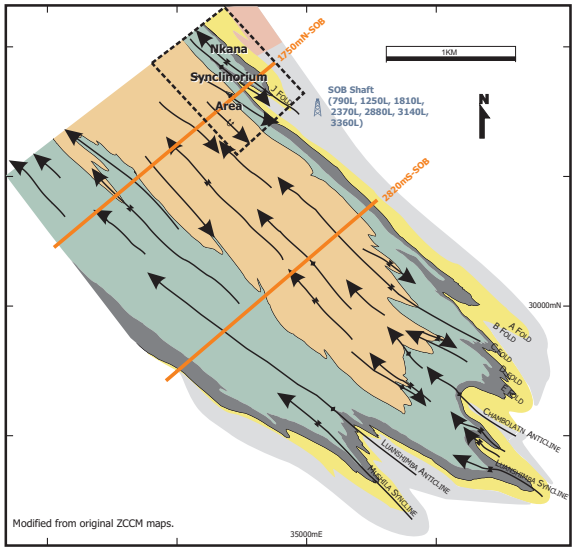

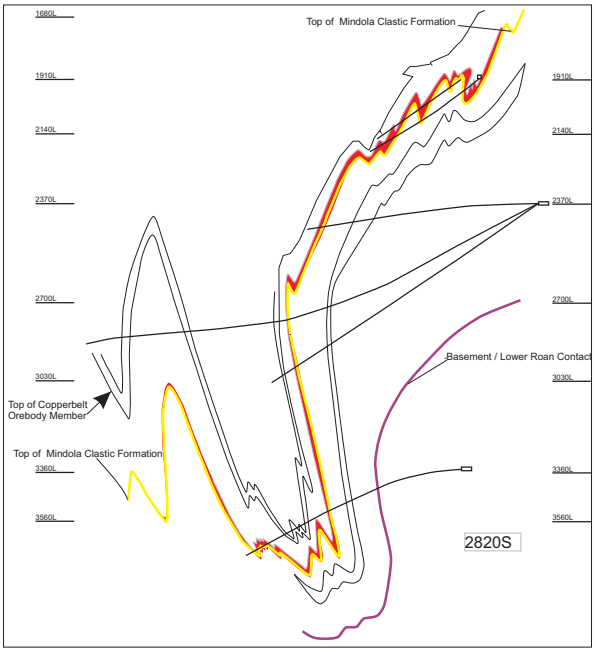

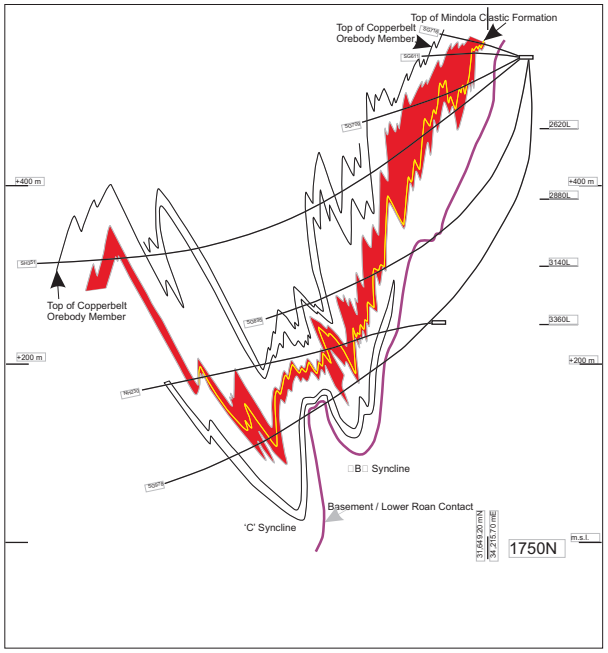

Figure 5.11. Geometry of the copper orebody in the southern part of the NKM deposit. The orebody is within the moderate and high strain structural domains and is hosted within the lower portion of the carbonaceous-carbonate argillite facies association COM 2. Chalcopyrite + pyrite + carrollite are the main sulphide phases disseminated throughout the copper orebody, as well as hosted within veins which are confined within the overall copper orebody geometry (Sections compiled from historic mine data).

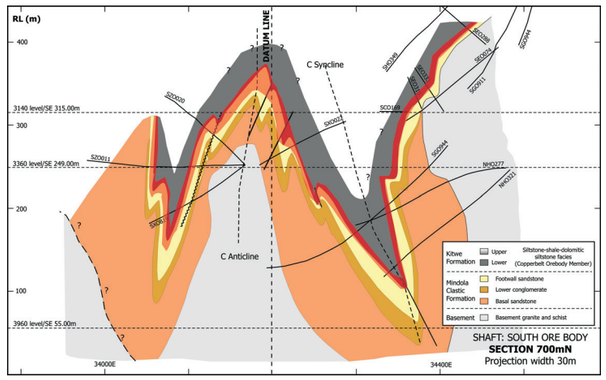

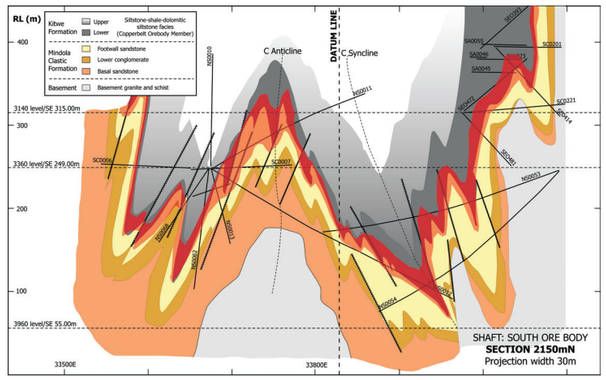

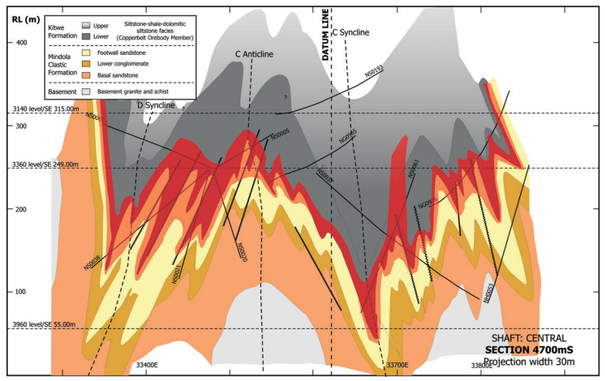

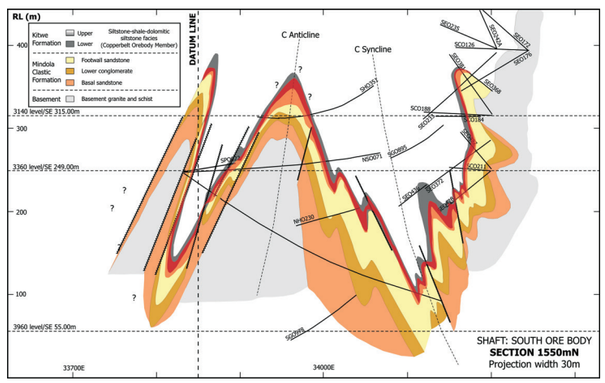

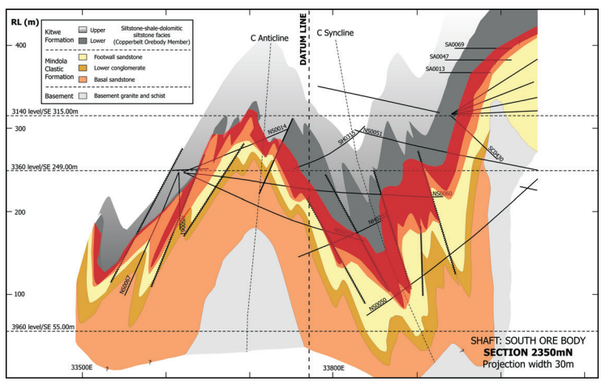

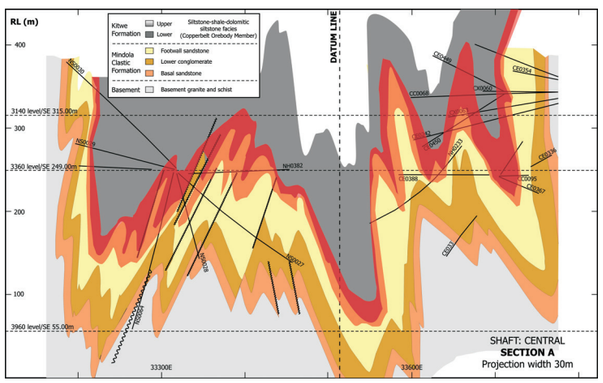

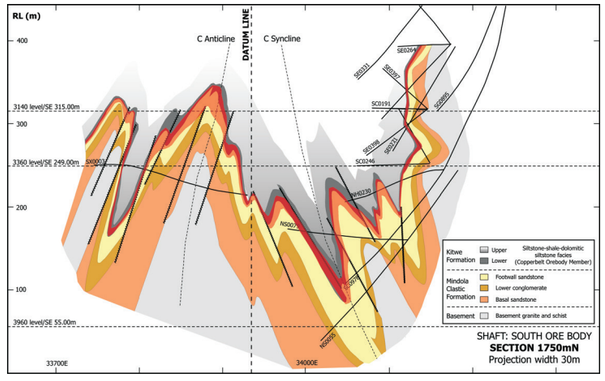

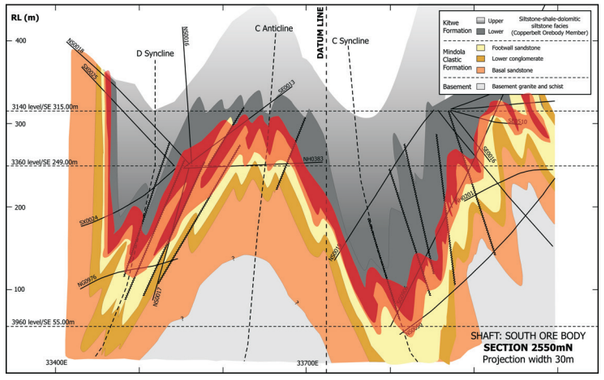

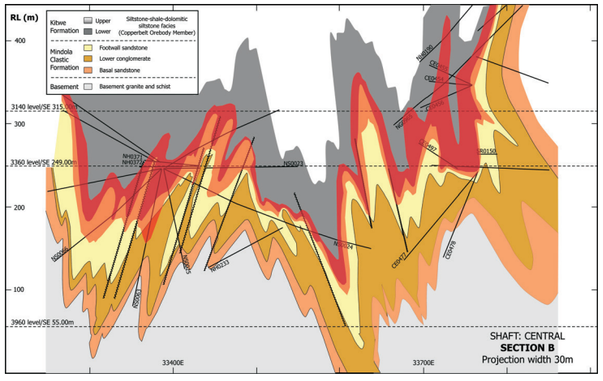

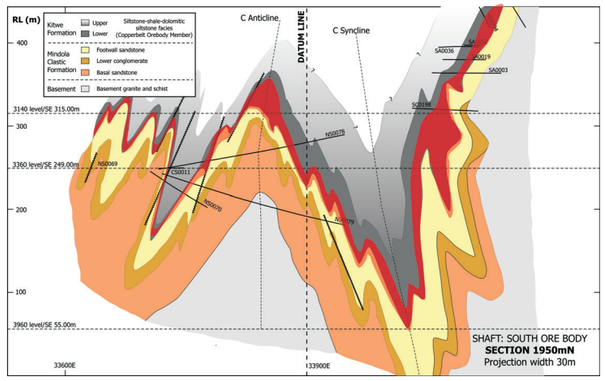

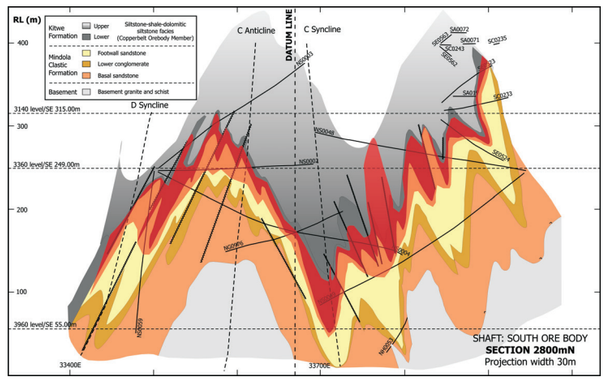

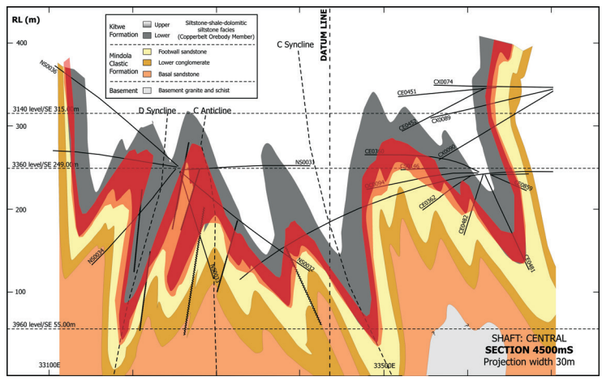

Figure 5.12. Geological sections with the copper orebody overlayed (>0.5 % Cu) for the Nkana Synclinorium Area. Digital Appendices 3 and 4 contain the A0 original hand drawn interpretation sections and level plan maps. The ~70m spaced simplified geological sections for the Nkana Synclinorium Area (looking northwest) were constructed from geological map data and drillhole interpretation. The 'C' syncline and anticline are well defined. Significant structural thickening of the COM and the Cu orebody occurs in the hinge zone of the folds. Late stage faulting further complicates the mesoscale fold geometry. The sections are displayed from bottom left to bottom right moving from SE to NW, down plunge along the 'C' syncline. The copper orebody is folded and there is thinning on the fold limbs and thickening of the orebody particularly associated with the 'C' anticline.

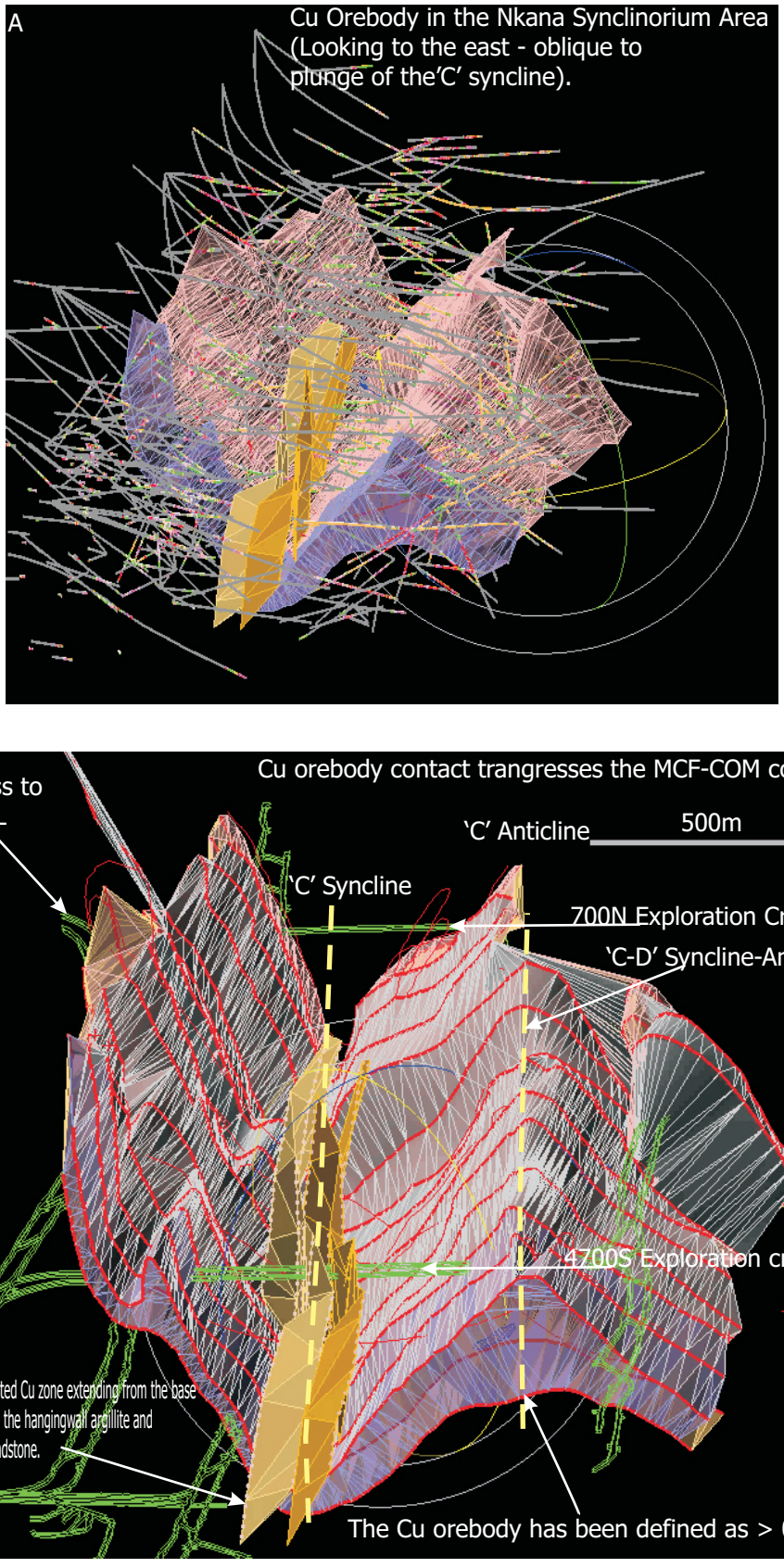

Figure 5.13. Three dimension interpretation of the copper Orebody within the Nkana Synclinorium Area at SOB Shaft using drillhole data to constrain ore envelope. Three dimensional modelling of the orebody was constructed by the author using Vulcan. The cut-off for the copper ore envelope was 0.5% Cu a). Oblique view of the copper orebody, looking to the south. b). Looking to the south along the axis of the 'C' syncline. The copper orebody is stratabound and does transgress the MCF-COM contact, although over ~80% of the copper orebody is hosted by the COM. The yellow surfaces depict an interpreted small sheared hosted zone of mineralization extending from the basal portion of the COM into the hangingwall argillite. This is atypical of the overall copper orebody at NKM and cannot be traced laterally for more than a few hundreds of metres and does not cross cut lower levels of the stratigraphy below the COM. It is interpreted as structural controlled remobilised copper ore shoot. Refer to digitial Appendix 6 for complete Vulcan files as well as digitial movie of the orebody.

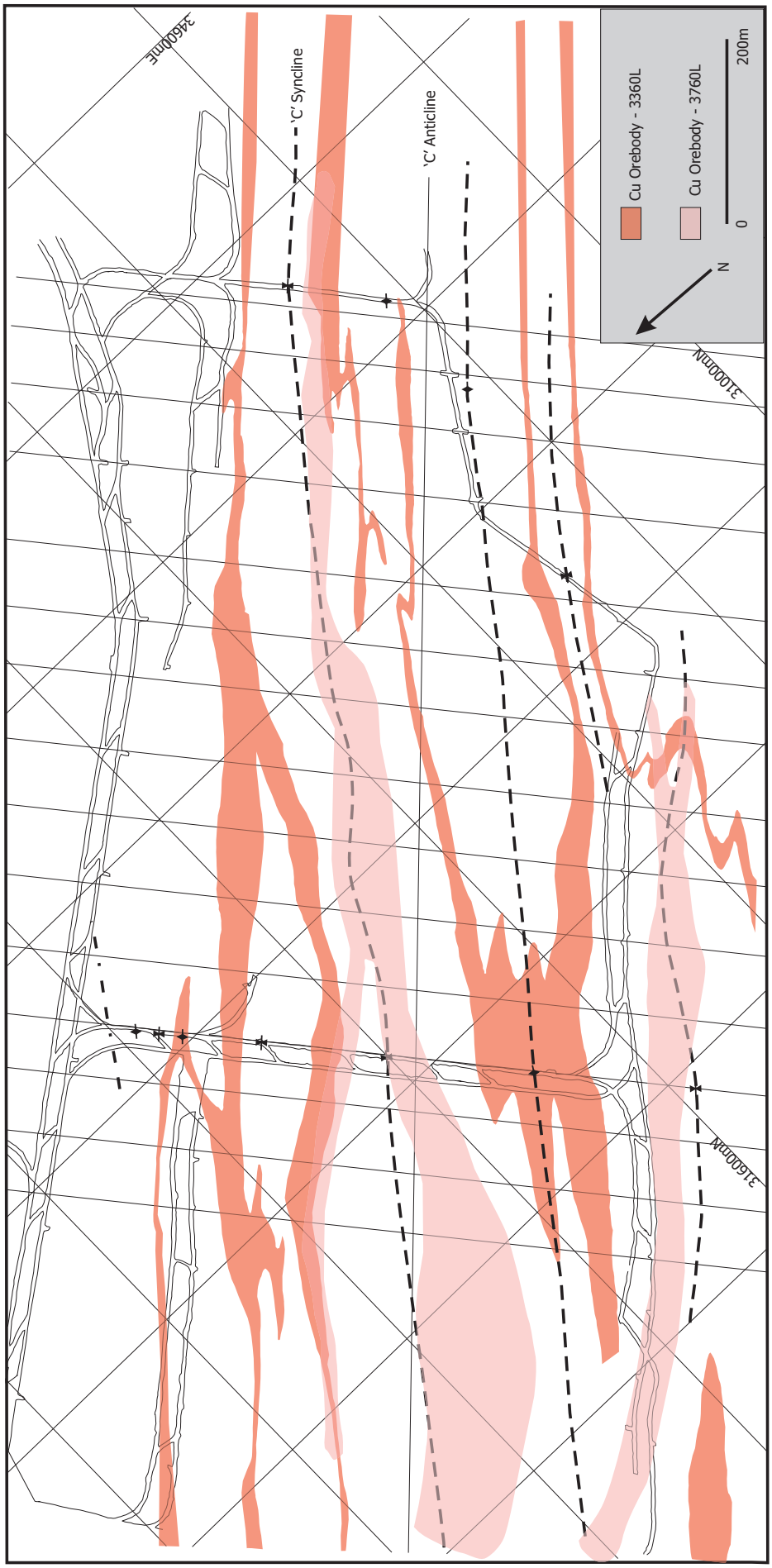

Figure 5.14. Level plan of the 3360L and projected 3760L showing only the geometry of the copper ore envelope (>0.5% Cu) constructed from pierce points through each level. The density of data prevents an accurate construction of copper orebody outline on the 3760L however the construction of the basic three dimension copper orebody, in combination with this map, shows the copper orebody is grossly stratabound within the high strain structural domain at NKM.

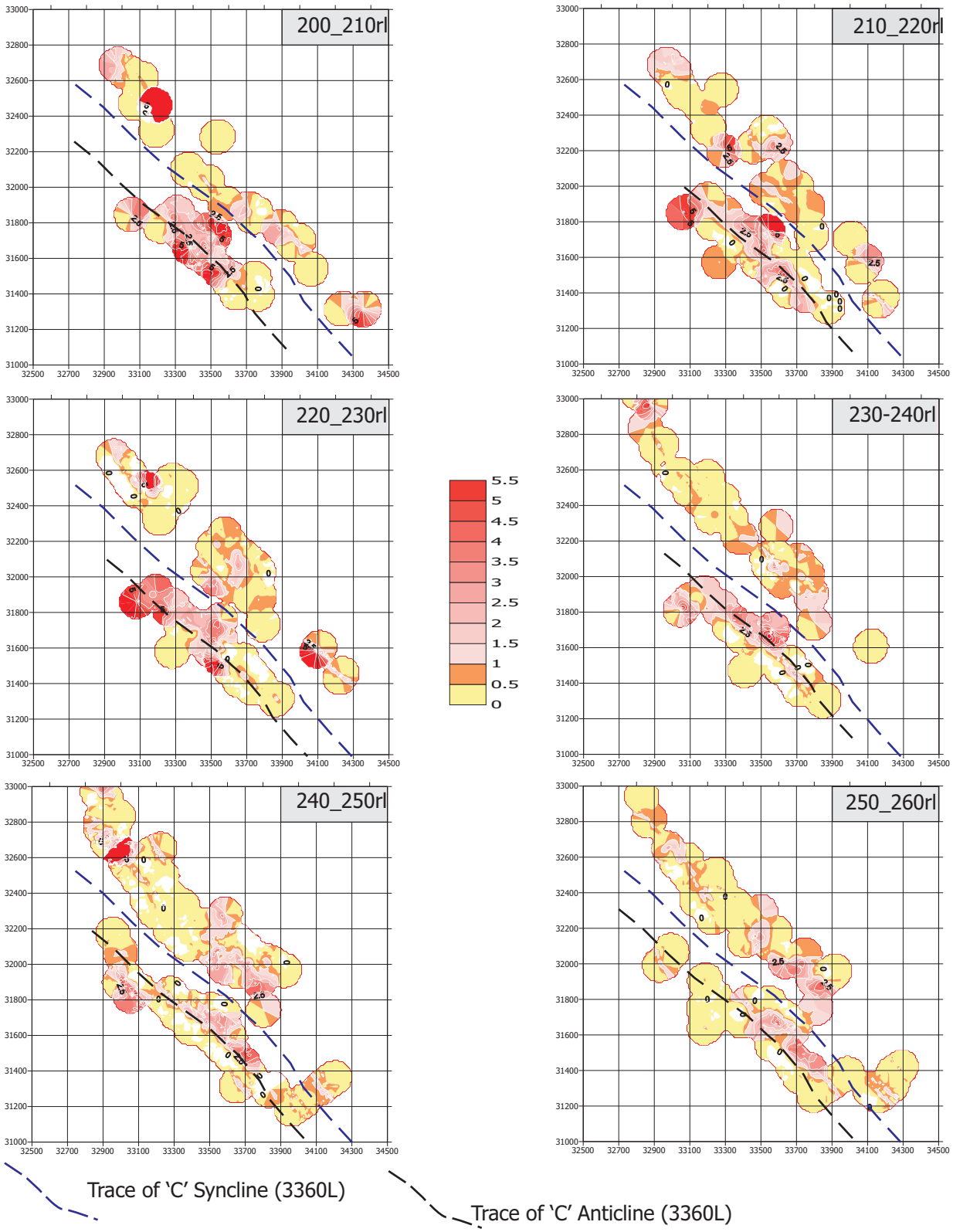

Figure 5.15. Contoured copper grade level plans from the Nkana Synclinorium Area. Each slice is 10m thick. The 3360L, from which all geological mapping was conducted, is the 240 to 250rl. The trace of the 'C' syncline and anticline on the 3360L have been marked on each level plan. Contouring was conducted using inverse distance and confined between the assay hanging and footwalls. The gross geometry of the 'C' syncline is clearly visible, however the lack of data points on the western limb of the 'C' anticline does not allow for accurate contouring of grade data in two dimensions. Refer to digital appendix 7 for complete contouring data for the Nkana Synclinorium area.

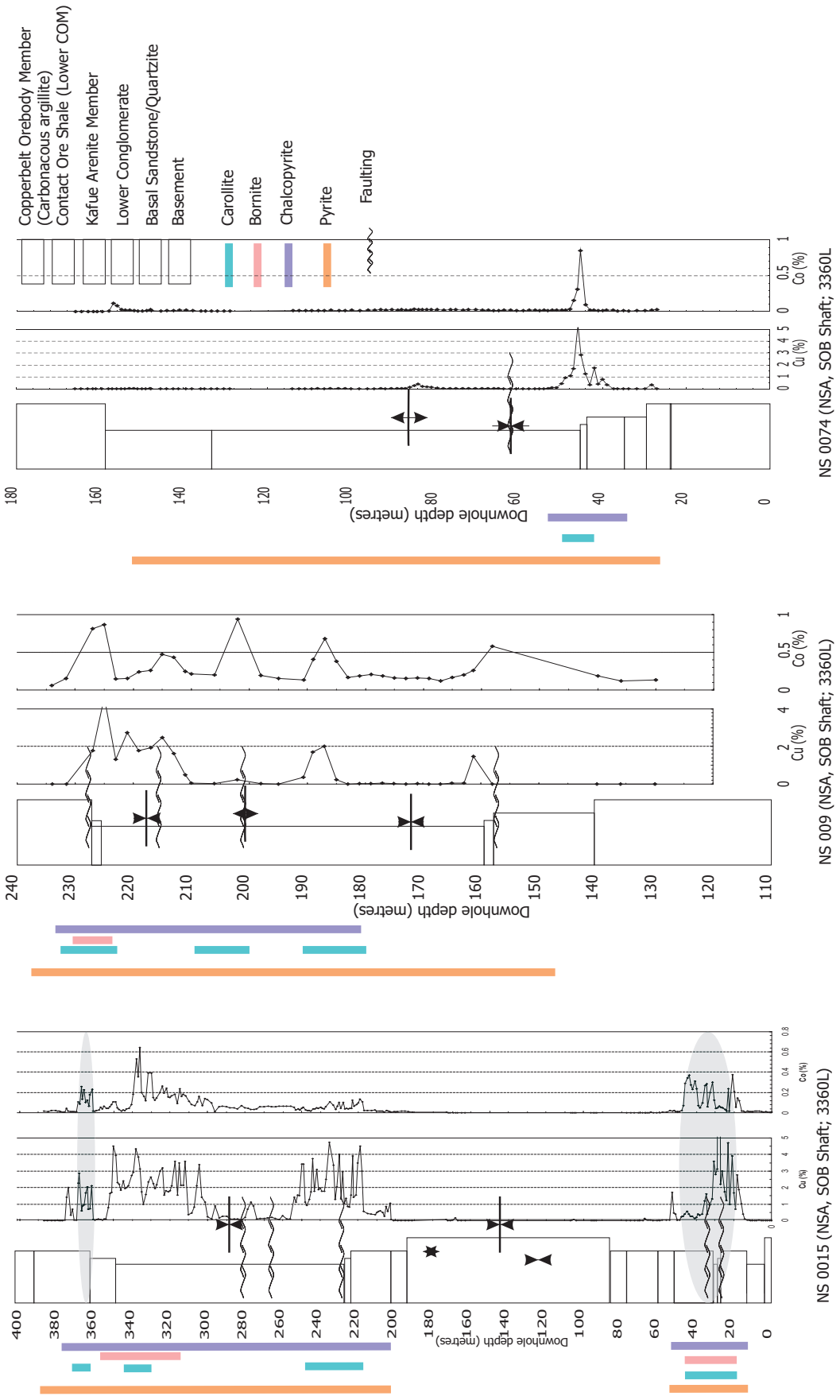

Figure 5.16. Simplified geological logs, downhole grade plots and sulphide distribution of three drillholes from within the Nkana Synclinorium Area. Copper mineralisation >0.5% is confined to the upper 10m of the MCF and the lower 10m of COM. Chalcopyrite is main copper sulphide. Minor amounts of bornite are typically associated with the upper MCF, S3 parallel and cross cutting vein generations. Dolomite-Quartz-Sericite-chalcopyrite-bornite veins are common within the high strain domain, however are confined within the overall folded stratabound copper ore envelope.

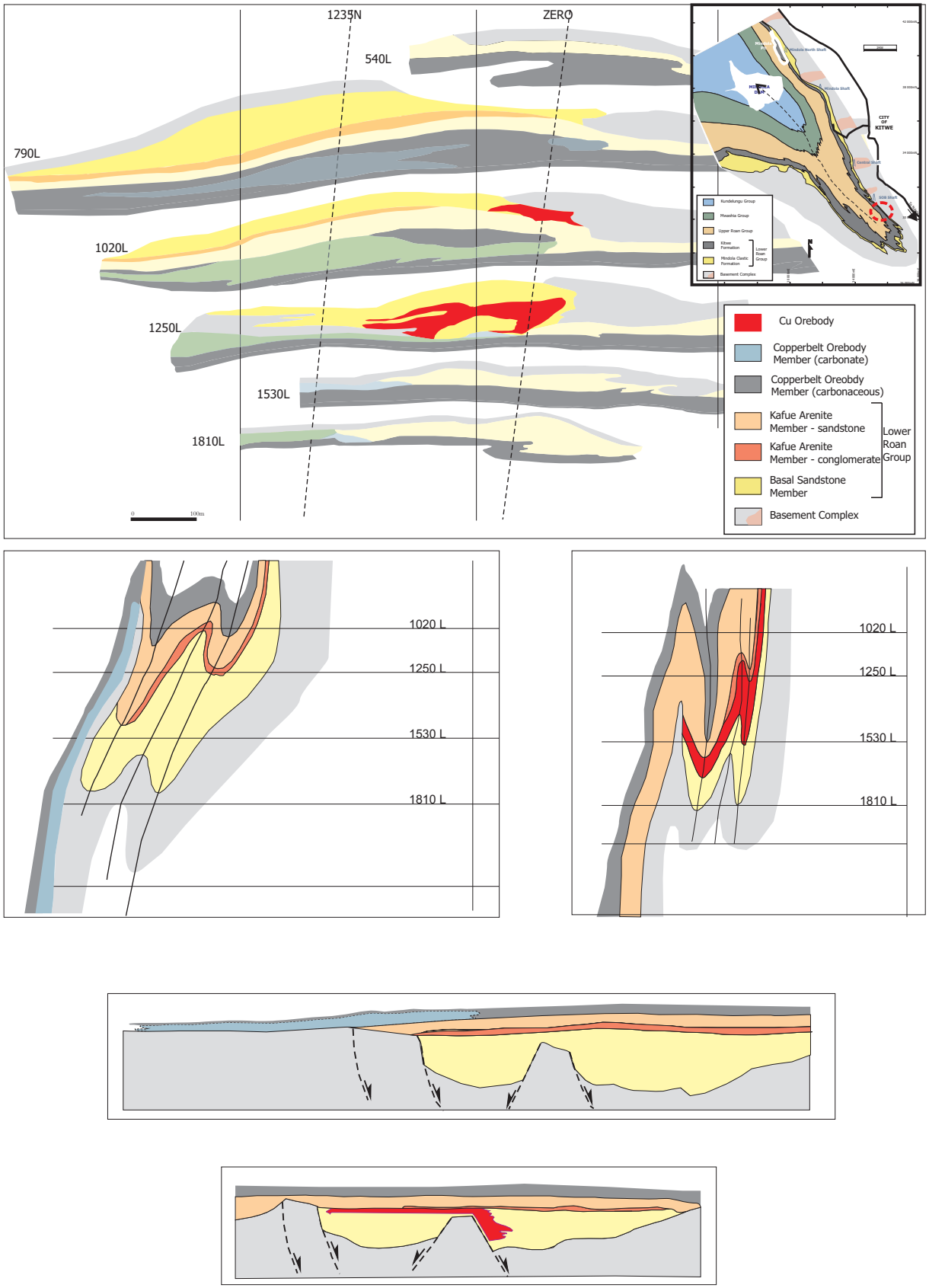

Figure 5.17. Schematic plan maps, sections and unrolled sections for the Basal Quartzite Orebody at SOB Shaft. The data was compiled from historic datasets and those of Richards (1965). The copper mineralisation is hosted in lower portion of the MCF. The orebody was mined out during the 1960's therefore the area was not accessible during this study. The schematic interpreted "unrolled" sections suggest the copper mineralisation was associated with a small syn-rift basin compartment, similar to the well documented Chibuluma B deposit (Selley et al., 2002; 2005) as depicted in Figure 5.2, however it is noted there are some discrepancies in the thickness of the MCF.

were synchronous events.

Sulphide mineralisation along bedding planes and foliation is common, although it is difficult to ascertain the extent of deformation accommodated by simple shear along bedding plane, and to what extent it accompanied syn-tectonic mineralisation or remobilisation of sulphides. The amount or rate of movement on bedding planes is unknown as repeated deformation and recrystallisation of sulphides and gangues suggests sulphide remobilisation accompanied simple shear between sedimentary strata.

Within the upper portions of the carbonaceous argillite, intervals containing elongated nodules of carbonate, anhydrite, quartz and sulphides occur and are similar to those observed in the northern domain (Figs 5.19e and 5.19f). The proportion of carbonate appears to decrease approaching the assay hangingwall contact, coinciding with an increase in anhydrite. The anhydrite lenses are deformed, exhibiting elongation parallel to S_3.

5.7 MICROSCOPIC TEXTURAL VARIATION AND SULPHIDE PARAGENESIS

Ore textures and their relationship to gangue mineralogy provide valuable information to assist with defining the timing of mineralisation relative to the formation of penetrative fabrics and metamorphism possibly affecting the distribution of the different sulphide phases. The following section describes textural observations of the main copper sulphide assemblage. A small complimentary pyrite chemistry study is used to address specific questions relating to internal zoning which cannot be identified by petrographic means. Within the moderate to highly deformed portions of the deposit, there is considerable evidence for metamorphic segregation and recrystallization having resulted in repartitioning of sulphides and gangue minerals into bands, cleavages, veins, and lenses. The proposed paragenetic sequence refers to the observed sulphide assemblages and textures (Table 5.5). However it is important to note that recrystallization associated with upper-greenschist facies metamorphism has occurred; therefore it is difficult to determine from textural studies alone certain early stage relationships prior to the onset of deformation and metamorphism

5.7.1 Pyrite – (FeS_2) (Figs 5.23 and 5.24)

Pyrite is the most common and widespread sulphide phase in the southern part of the main copper orebody and within zones of sub-economic mineralisation along the western limb of the Nkana Syncline. In the northern part pyrite occurs within the upper portion of the moderately dipping orebody. Within the hangingwall portion of the COM, pyrite is distributed across the NKM area and is hosted in a carbonaceous-calcareous argillite.

Pyrite occurs in a variety of forms, likely recording temporally distinct episodes of growth, however when in association with other sulphide phases, it is commonly paragenetically the earliest. All forms of pyrite are observed being overgrown by chalcopyrite, carrollite and accessory sulphides including sphalerite. Pyrite grains typically exhibit colour variation from browny-cream to typical white-cream colour. No framboidal pyrite was identified during this study, however such textures have been documented in several internal ZCCM mineralogical reports at NKM and in a study by McGoldrick and Cooke (2003). Type 1 pyrite occurs as very fine (~0.1mm or less) disseminated grains in carbonaceous argillite, accounting for ca. 20% of the total pyrite occurring in the copper orebody, and ca. 15% of the total pyrite within assay hangingwall carbonaceous argillite (Fig. 5.23a). In high strain zones, 0.2 to 1 cm inclusion free, rotated, type 2 pyrite poryhroblasts with strain shadows of quartz-calcite are common and account for ca. 20% of the total observed pyrite (Fig. 5.23c). No pressure shadows have been observed associated with chalcopyrite, carrollite or bornite presumably because these are mechanically weaker phases. Type 3 pyrite has inclusions of mica laths which in some cases are aligned parallel to the regional foliation, or may exhibit a random orientation (Fig 5.23d). This type of pyrite is

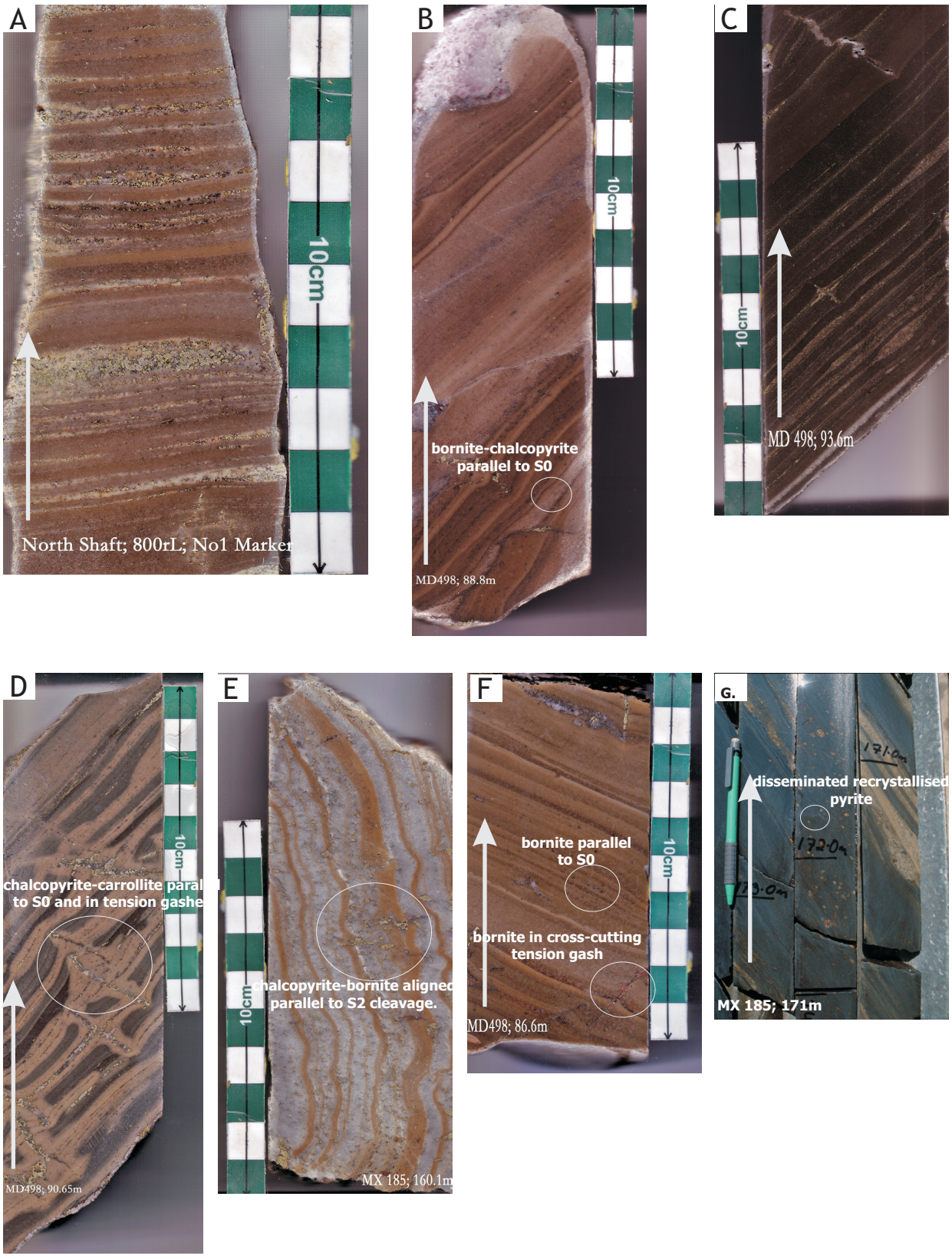

Figure 5.18. Hand specimen samples of sulphides hosted in dolomite-argillite dominated lithologies of the northern domain at NKM, low strain domain: a). Disseminated bornite and minor chalcopyrite hosted in the Banded Ore. (North Shaft) b). Disseminated chalcopyrite and bornite hosted in Low Grade argillite to Banded Ore Units. There is an increase in sulphides associated with coarser grained layers. (MD 498; 88.8m). Anhydrite and dolomite is common in these intervals. c). Chalcopyrite-carrollite hosted in argillite, sulphides disseminated within individual beds and as aggregates cross-cutting bedding. MD 498; 93.6m) d). No 1 Marker (mine terminology), chalcopyrite dominate, sulphides aligned parallel to S2 cleavage (MD498; 90.5m) e).Banded Ore (mine terminology) hosting disseminated bornite and carrollite as well as chalcopyrite aggregates cross-cutting bedding (Mx185; 160.1m) f). Disseminated bornite and bornite within fractures hosted in the Low Grade Argillite unit (MD 498; 86.6m). g). Hangingwall Argillite (mine terminology) with disseminated pyrite commonly associated with anhydrite nodules.

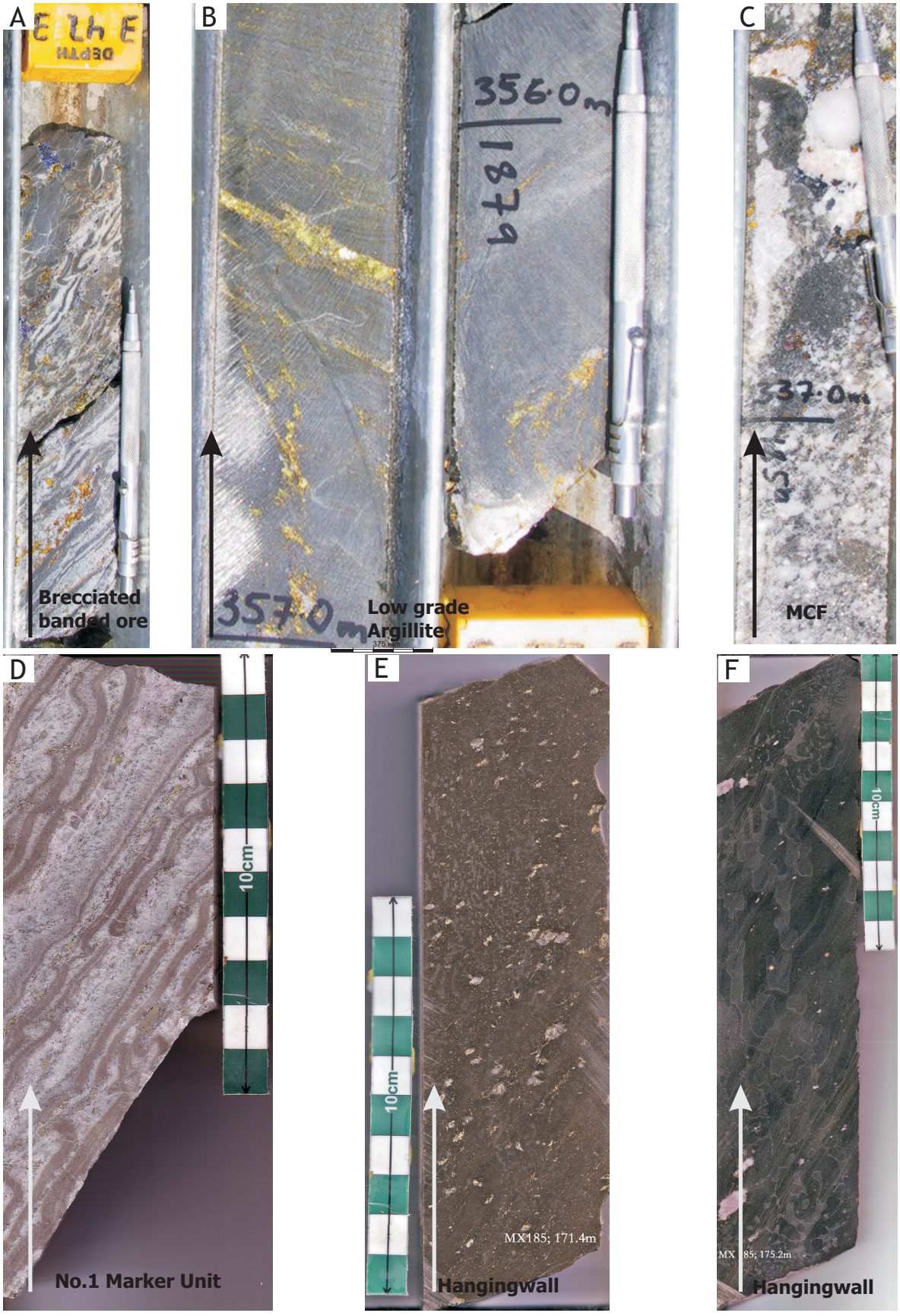

Figure 5.19. Examples of copper sulphides hosted in the dolomite-argillite rock of the northern part of the orebody, at deeper levels, in moderate strain domain. a). Brecciated Banded Ore of bornite-chalcopyrite from the deeper levels at Mindola Shaft (MX 182; 347m); b). Chalcopyrite aligned parallel to S3 and locally concentrated in veining within the Lower Argillite unit (MX 182; 357m); c). Disseminated chalcopyrite-bornite within the upper portion of the MCF (MX 182; 337m); d). No 1. Marker dolomite-calcite-anhydrite with disseminated chalcopyrite-bornite (MX 182; 350m); e). Hangingwall argillite unit with disseminated pyrite (MX 185; 171.4m); f). Hangingwall argillite unit with anhydrite-calcite nodules and disseminated pyrite (MX 185; 175.2m).

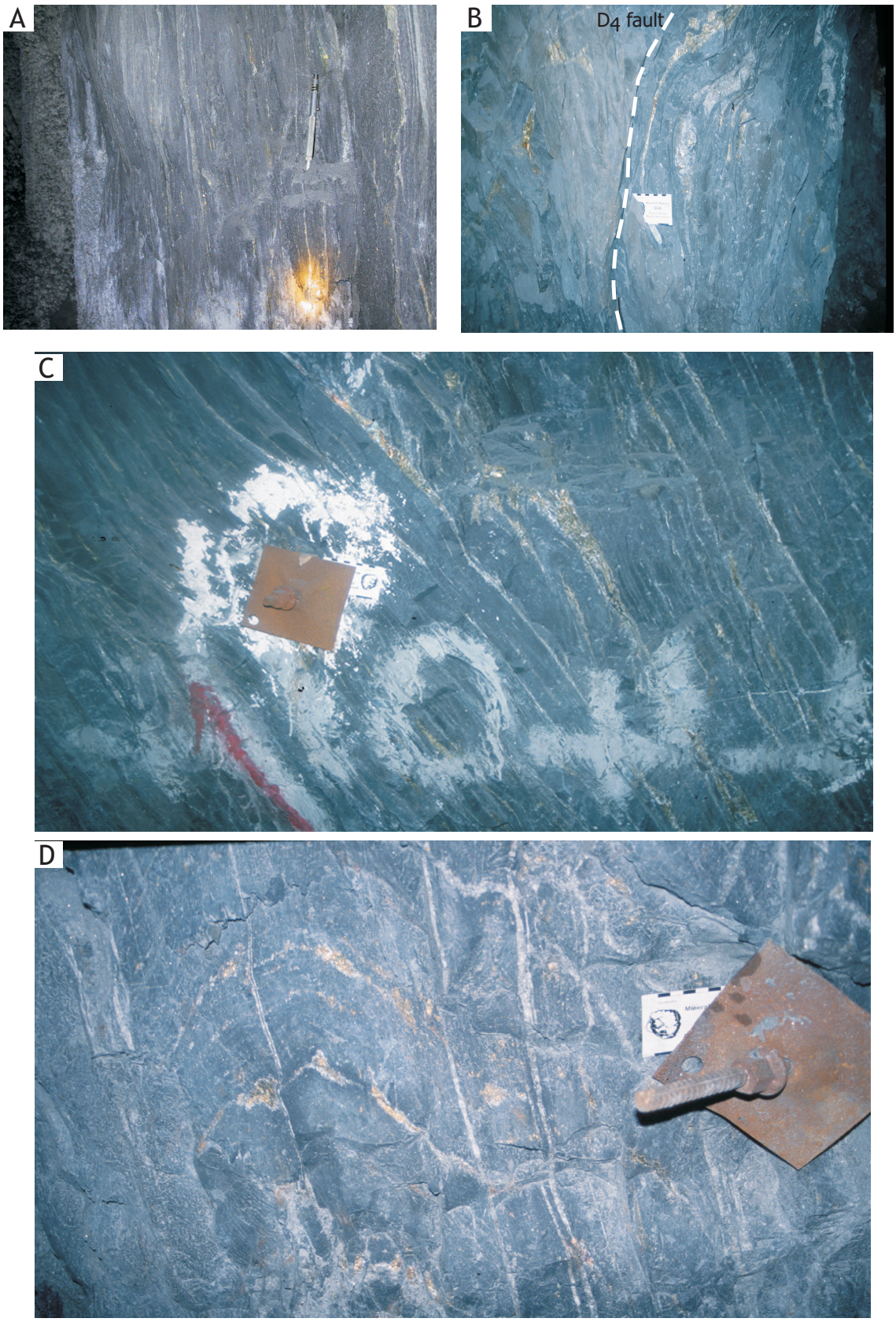

Figure 5.20. Underground photos from the 3360L Nkana Synclinorium Area at SOB Shaft. a). Disseminated chalcopyrite-pyrite aligned parallel to S3 cleavage. b). Chalcopyrite concentrated parallel to S3 which has been locally folded due to D4 faulting. c and d). Examples of disseminated chalcopyrite and vein hosted chalcopyrite.

Figure 5.21. All samples from the southern mineralised domain, within the transition from dolomite-argillite to carbonaceous argillite. a). Chalcopyrite-carrollite ore from the lower portion of the COM at SOB Shaft. (NSA, 3360L, SOB Shaft). b). Chalcopyrite dominate recrystallised parallel to main cleavage within a biotitic argillite (NSA,3360L, SOB Shaft). c). Disseminated chalcopyrite hosted in dolomitic argillite. (2230L, Central Shaft). d). Chalcopyrite-carrollite aligned to S3 cleavage, within dolomitic argillite rock from the facies transition zone (CX187, Zero Anticline, Central Shaft).

interpreted to have formed syn-D_3 and is widely distributed throughout the copper orebody, particularly in the southern domain. Type 4 pyrite are characterised by internal zonation from anhedral yellowish inclusion-rich cores to euhedral whiter 'cleaner' rims (Fig. 5.23e). It is observed within the copper orebody envelope, yet lacks even distribution, or systematic relationship to either lithotype or deformation style. The dissolution and partial replacement of pyrite by pyrrhotite along cleavage and fracture planes results in remnant pyrite grains enclosed within a matrix of pyrrhotite and within the high strain domain, pyrite and pyrrhotite may occur together (Fig. 5.23f). No pyrite has been identified intergrown with bornite or chalcocite at NKM. Euhedral pyrite grains, occur as the sole sulphide phase along the margins of the carbonate facies barren gaps, when in association with the carbonaceous-carbonate argillite facies association in the southern part of the orebody.

Pyrite Chemistry

The internal zonation of pyrite grains, as typified by type 4 pyrite at NKM, has long been recognised at certain ZCB deposits (e.g. Annels, 1970; Simmonds, 1980, Annels and Simmonds, 1984; Table 5.3). Simmonds (1980) documented enrichments of trace elements (Co and Ni mainly) within pyrites from the Luanshya deposits. These variations can be related to different generations of the mineral and to the existence of equilibrium assemblages of carrollite, chalcopyrite and pyrite. Beyond the ZCB, pyrite has been identified as a sink for Co and Ni which substitute for Fe (Vaughan and Craig, 1978; Craig et al., 1979). The cobaltiferous pyrite belongs to the isomorphous series pyrite-cattierite (CoS_2) and Abraitis et al. (2004) showed that approximately 12 mol% CoS_2 is soluble in pyrite at 400°C and by 700°C solid solution between cattierite and pyrite is complete. Jordaan (1961) described zoned pyrites from the southern part of the NKM orebody that vary from creamy white to pinkish brown and have differences in polishing hardness and reflectance, documenting that the brown coloured zones contain lower amounts of cobalt than the paragenetically later white zones. Similar pyrites have been observed during this study (Fig 5.23e) and the high cobalt pyrite appears to only exist in association

Table 5.3. Cobalt poor and cobalt rich pyrites have previously been documented by Simmonds and Annels (1984) at several other deposits on the ZCB.

Analytical Data from Simmonds and Annels (1984)

		Electron Microprobe Analysis (wt%)					
Location	**Sulphide**	**Fe**	**Co**	**Ni**	**Cu**	**S**	**Total**
Baluba	Pyrite	47.59	0.84		0.36	49.04	97.86
Baluba	Co-Pyrite	38.82	11.75		0.11	49.88	98.61
Baluba	Co-Pyrite	34.81	13.66		0.18	49.35	97.99
Baluba	Chalcopyrite	31.22	0.61	0.04	35.54	32.02	99.42
Baluba	Co-pyrite	38.46	10.11	0.11	0.8	51.59	101.06
Baluba	Co-pyrite	29.07	19.14	0.28	0	51.41	99.91
Baluba	Carrollite	0.25	39.88	0.49	19.79	40.7	101.1
Baluba	Carrolite	0.25	37.95	0.48	21.92	41.36	101.95
Baluba	Chalcocite	3.18	1.27	0.07	72.95	19.45	96.92
Baluba	Co-pyrite	41.73	7.57	0.14	0	50.89	100.34
Baluba	Chalcopyrite	31.16	0.47	0.05	34.84	33.72	100.24
Baluba	Chalcopyrite	30.94	0.55		35.55	32.07	99.16
Baluba	Carrollite	0.82	42.52	0.52	17.06	40.45	101.36
Chibuluma	Chalcopyrite	32.07	0.49		35.59	32.38	100.54
Chibuluma	Co-pyrite	38.12	11.55		0.65	48.54	98.86
Chibuluma	Carrolite	0.58	37.98	2.53	19.37	39.61	100.06
Chibuluma	Carrollite	0.69	39.04	0.59	19.95	39.43	99.71
		0.82	38.88	0.45	20.2	40.02	100.36
Chibuluma	Carrolite +	0.51	37.57	0.86	20.82	39.8	99.56
Chibuluma	chalcopyrite-bornite	0.49	36.86	1.04	21.12	39.35	98.86

with carrollite within the copper orebody (Table 5.3). Simmonds (1980) identified similar pyrites at the Baluba deposit and concluded there is no definitive and reproducible compositional variation in pyrite which can be correlated to stratigraphic position at the Baluba deposit.

Thirty-eight pyrite grains were analysed using a microprobe to determine the Co content of pyrite grains (Table 5.4). Eighteen of these grains were of type 4 pyrite and sampling included paired analyses of cores and rims. All samples were from highly strained southern part of the COM orebody at SOB shaft. Typically unzoned pyrite grains (Types 1 to 3) have no detectable levels of Co, whereas zoned pyrites have a rim enriched in Co relative to the core. These zoned pyrites contain up to ca. 4.5% Co on the crystal boundaries, between the core and rim, while more diffuse cobalt-enriched pyrite grains contain up to ca. 7% Co. The pyrite grains which have an enrichment of cobalt along rims are spatially closely associated with carrollite and chalcopyrite within the sample. In some cases the pyrite is partially replaced by carrollite. It is suspected the optical similarity between the cobaltiferous pyrite and carrollite commonly results in optical misidentification. The cobalt enriched pyrite has formed later than the cobalt-poor pyrite. Simmonds (1980) indicates the cobalt in pyrite is distributed as distinct and more diffuse zones and there is no systematic distribution at an intergranular scale and spatial throughout the deposit. Without a more extensive study comparing many samples from the northern and southern domains the same conclusions cannot be drawn from this limited study at NKM.

5.7.2 Chalcopyrite - $CuFeS_2$ (Figs 5.25, 5.27)

Chalcopyrite is the most widespread, and on average, most abundant Cu-sulphide at NKM. It is relatively evenly distributed throughout the carbonaceous argillite in the southern part of the COM orebody, but less so in the northern part, where bornite-dominant zones exist. The carbonaceous argillite hosts anhedral chalcopyrite grains that range from 30 to 50 microns in diameter, however vein-hosted chalcopyrite grains can be up to 2-4 mm in diameter (Fig. 5.25a). Chalcopyrite was particularly susceptible to local remobilization and has been folded in high strain zones. Typically chalcopyrite may occur as elongate crystal aggregates, locally including carrollite, bornite, pyrite, detrital quartz, and metamorphic phlogopite, occur aligned along deformed bedding lamellae or the S_2 cleavage (Figs 5.25b, 5.25d and 5.25f). Massive grain aggregates concentrate in microscopic fold hinges, consistent with syn-kinematic sulphide growth in micro-domains of low mean stress. Within the strongly folded portions of the orebody, where bedding is parallel to, and in many cases transposed by S_3, coarse-grained, elongate lozenges of chalcopyrite are aligned parallel to S_3 foliation and do not exhibit individual crystal orientation. Lozenges are up to 2 cm long and are separated by highly foliated carbonaceous argillite (Figs 5.25b and 5.25f). In some cases the edges of the chalcopyrite are intergrown with mica along the S_3 foliation and other sulphides such as bornite may exhibit the same features.

The Contact Ore Shale at the base of the COM hosts chalcopyrite grains which are frequently intergrown by silicates phases such as biotite and tremolite (Figs 5.27a-d). Chalcopyrite may have inclusions of pyrite and can display myrmekitic replacement, vermicular and exsolution lamellae textures with bornite (Fig. 5.27f). Chalcopyrite is seen enclosing pyrite (Fig. 5.27b) and can be overgrown (Fig. 5.27c). Inclusions of silicates within chalcopyrite are common. Within the upper portion of the mineralised MCF, chalcopyrite and bornite are within the matrix of calcite, dolomite, feldspar and quartz (Fig. 5.28g). Internal ZCCM reports refer to similar occurrences of chalcopyrite within the mined Basal Quartzite Orebody at SOB Shaft, however no mineralised samples were obtained from this area during this study. Chalcopyrite is replaced by secondary phases within the oxide zones of the orebodies.

Table 5.4. Analytical data from microprobe. Both cobalt poor and cobalt rich pyrites were identified at the NKM deposit. The cobalt rich pyrites have been highlighted in yellow.

Location	Mineral	Sample No.		Electron Microprobe Analysis (wt%)								
				Fe	Co	Ni	Cu	S	Zn	As	Se	Total
SOB Shaft	pyrite	253no2_py1	NS015_12.6m	48.96	0.00	0.01	0.02	53.80	0.00	0.00	0.02	102.81
SOB Shaft	pyrite	253no2_py10	NS015_12.6m	48.59	0.00	0.00	0.00	53.44	0.02	0.00	0.02	102.06
SOB Shaft	pyrite	253no2_py11	NS015_12.6m	48.47	0.00	0.00	0.02	52.73	0.00	0.00	0.02	101.24
SOB Shaft	pyrite	253no2_py12	NS015_12.6m	48.99	0.01	0.02	0.00	53.16	0.00	0.00	0.01	102.20
SOB Shaft	pyrite	253no2_py13	NS015_12.6m	48.81	0.00	0.03	0.02	53.50	0.02	0.00	0.02	102.41
SOB Shaft	pyrite	253no2_py14	NS015_12.6m	49.03	0.00	0.00	0.01	52.98	0.00	0.00	0.02	102.04
SOB Shaft	pyrite	253no2_py15	NS015_12.6m	49.11	0.00	0.00	0.01	53.40	0.00	0.00	0.02	102.54
SOB Shaft	pyrite	253no2_py2	NS015_12.6m	48.14	0.65	0.01	0.02	53.48	0.01	0.00	0.03	102.34
SOB Shaft	pyrite	253no2_py3	NS015_12.6m	47.89	0.49	0.05	0.01	53.01	0.00	0.00	0.02	101.47
SOB Shaft	pyrite	253no2_py4	NS015_12.6m	48.19	0.01	0.04	0.00	53.23	0.00	0.00	0.03	101.50
SOB Shaft	pyrite	253no2_py5	NS015_12.6m	43.71	5.21	0.01	0.03	52.99	0.00	0.00	0.00	101.95
SOB Shaft	carrollite	253no2_py6	NS015_12.6m	31.96	17.59	0.00	0.08	53.07		0.01	0.00	102.72
SOB Shaft	pyrite	253no2_py7	NS015_12.6m	48.43	0.03	0.08	0.03	53.34	0.00	0.00	0.01	101.93
SOB Shaft	pyrite	253no2_py8	NS015_12.6m	48.58	0.00	0.01	0.00	53.11	0.00	0.00	0.01	101.71
SOB Shaft	pyrite	253no2_py9	NS015_12.6m	48.96	0.01	0.00	0.02	53.25	0.00	0.00	0.03	102.26
SOB Shaft	pyrite	253no2_py10	NS015_12.6m	48.55	0.02	0.04	0.00	53.10	0.03	0.00	0.02	101.76
SOB Shaft	pyrite	253no2_py11	NS015_12.6m	48.83	0.02	0.17	0.00	53.40	0.01	0.00	0.03	102.46
SOB Shaft	pyrite	284_py1	NS015_299.8m	44.65	4.13	0.00	0.00	52.08	0.03	0.96	0.03	101.88
SOB Shaft	pyrite	284_py10	NS015_299.8m	45.91	3.17	0.01	0.00	52.24	0.01	0.54	0.02	101.91
SOB Shaft	pyrite	284_py11	NS015_299.8m	48.57	0.00	0.01	0.01	52.59	0.00	0.00	0.03	101.21
SOB Shaft	pyrite	284_py12	NS015_299.8m	48.74	0.01	0.00	0.00	52.65	0.05	0.00	0.02	101.47
SOB Shaft	pyrite	284_py13	NS015_299.8m	44.87	4.04	0.00	0.00	52.15	0.02	0.91	0.02	102.02
SOB Shaft	pyrite	284_py14	NS015_299.8m	48.60	0.03	0.00	0.00	52.42	0.00	0.00	0.02	101.08
SOB Shaft	pyrite	284_py16	NS015_299.8m	41.74	7.07	0.04	0.04	52.72	0.00	0.40	0.01	102.02
SOB Shaft	pyrite	284_py17	NS015_299.8m	41.88	7.11	0.04	0.06	53.13	0.04	0.39	0.02	102.66
SOB Shaft	pyrite	284_py18	NS015_299.8m	48.59	0.03	0.01	0.02	53.15	0.01	0.00	0.01	101.83
SOB Shaft	pyrite	284_py19	NS015_299.8m	43.59	4.63	0.01	0.01	51.95	0.00	1.08	0.04	101.30
SOB Shaft	pyrite	284_py2	NS015_299.8m	48.86	0.08	0.04	0.02	52.91	0.00	0.00	0.03	101.94
SOB Shaft	pyrite	284_py20	NS015_299.8m	45.18	3.92	0.00	0.00	52.98	0.02	0.08	0.02	102.20
SOB Shaft	pyrite	284_py21	NS015_299.8m	48.65	0.01	0.00	0.01	52.72	0.02	0.00	0.02	101.43
SOB Shaft	pyrite	284_py3	NS015_299.8m	44.52	4.27	0.02	0.01	52.13	0.01	1.02	0.02	102.01
SOB Shaft	pyrite	284_py4	NS015_299.8m	49.16	0.00	0.00	0.01	53.05	0.00	0.00	0.02	102.24
SOB Shaft	pyrite	284_py5	NS015_299.8m	45.04	3.83	0.00	0.00	52.09	0.00	0.77	0.03	101.76
SOB Shaft	pyrite	284_py6	NS015_299.8m	48.48	0.01	0.00	0.00	53.02	0.01	0.00	0.02	101.54
SOB Shaft	pyrite	284_py7	NS015_299.8m	44.86	3.63	0.01	0.00	52.37	0.00	0.76	0.03	101.67
SOB Shaft	pyrite	284_py8	NS015_299.8m	48.61	0.04	0.00	0.01	53.12	0.06	0.00	0.02	101.86
SOB Shaft	pyrite	284_py9	NS015_299.8m	44.44	4.23	0.01	0.00	51.90	0.00	1.06	0.01	101.66

Yellow shaded notes pyrite grains with internal cores of low cobalt and external rims enriched in the cobalt.
Grey shaded analysis is of a grain of carrollite mistaken for pyrite.

5.7.3 Bornite - Cu_5FeS_4 (Fig. 5.26)

The lateral distribution of bornite is restricted in comparison to chalcopyrite and pyrite. Bornite is rarely observed within the carbonaceous argillite of the COM at SOB Shaft, however is common within the equivalent dolomite-argillite sequence of the COM in the nothern area. Disseminated fine blebs of bornite are rarely observed within the carbonaceous argillite (Fig 5.26b). Chalcopyrite and bornite commonly occur in grain contact, however mutual intergrowth textures or opposing senses of overgrowth make it difficult to establish a consistent paragenesis (Fig. 5.26c). Exsolution textures of bornite in chalcopyrite, likely of high temperature origin (Craig and Vaughan, 1993), occur in highly strained samples (Fig. 5.26f). Two types of bornite are distinguishable by colour and their sulphide associations (Figs 5.26d and 5.26e). One of the bornite phases has a distinct brown-orange colour may have exsolved rims and laths of chalcopyrite. The other variant is reddish-brown and appears to be in mutual contact with the chalcopyrite (Figs 5.26d and 5.26e*)*. The reddish-brown phase of bornite may have exsolved chalcocite as well as pseudo-eutectic intergrowths with bornite. In the southern area of NKM bornite occurs in association with chalcopyrite and carrollite within the Contact Ore Shale and in the upper portions of the MCF (Figs 5.27g and 5.27h).

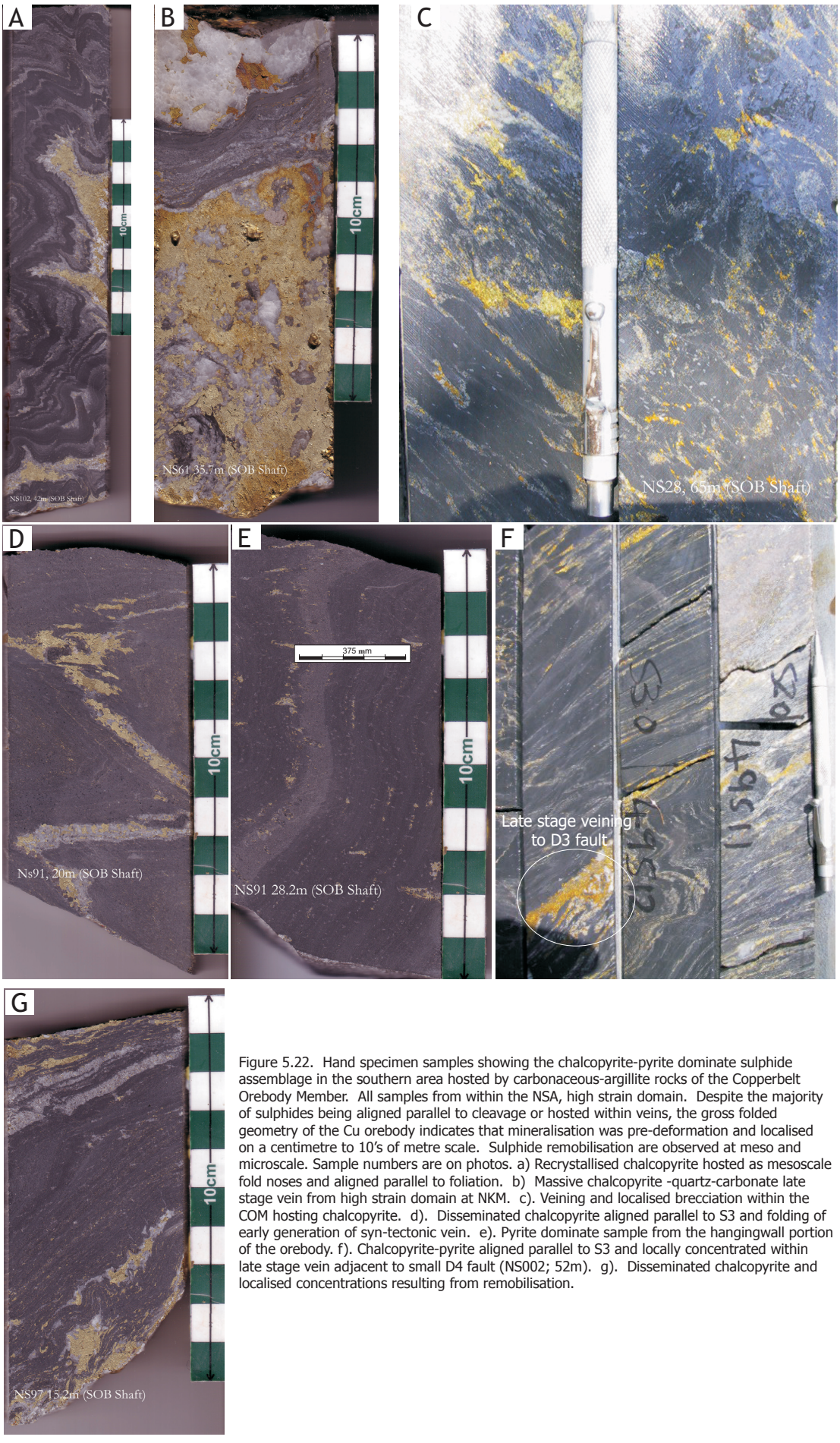

Figure 5.22. Hand specimen samples showing the chalcopyrite-pyrite dominate sulphide assemblage in the southern area hosted by carbonaceous-argillite rocks of the Copperbelt Orebody Member. All samples from within the NSA, high strain domain. Despite the majority of sulphides being aligned parallel to cleavage or hosted within veins, the gross folded geometry of the Cu orebody indicates that mineralisation was pre-deformation and localised on a centimetre to 10's of metre scale. Sulphide remobilisation are observed at meso and microscale. Sample numbers are on photos. a) Recrystallised chalcopyrite hosted as mesoscale fold noses and aligned parallel to foliation. b) Massive chalcopyrite -quartz-carbonate late stage vein from high strain domain at NKM. c). Veining and localised brecciation within the COM hosting chalcopyrite. d). Disseminated chalcopyrite aligned parallel to S3 and folding of early generation of syn-tectonic vein. e). Pyrite dominate sample from the hangingwall portion of the orebody. f). Chalcopyrite-pyrite aligned parallel to S3 and locally concentrated within late stage vein adjacent to small D4 fault (NS002; 52m). g). Disseminated chalcopyrite and localised concentrations resulting from remobilisation.

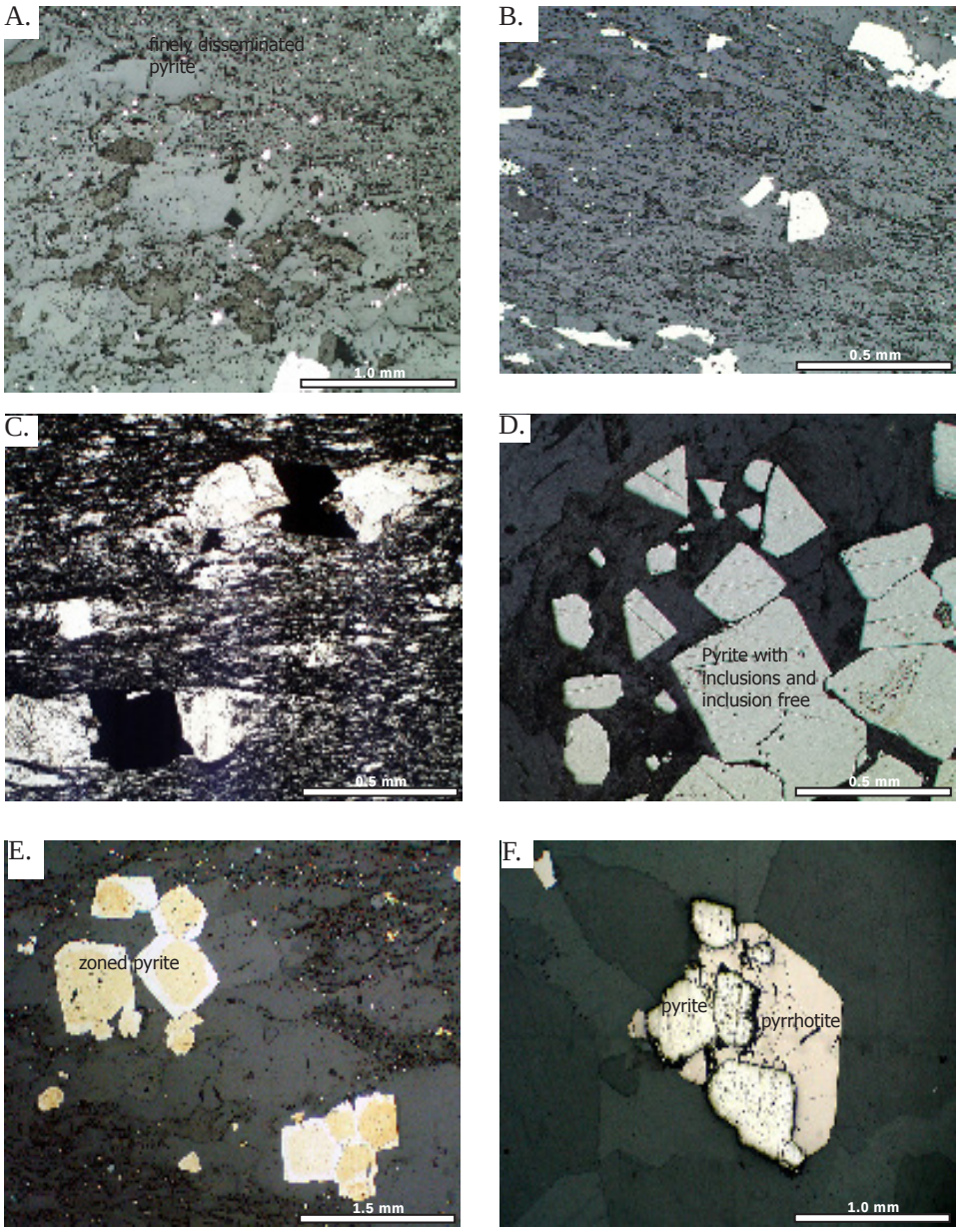

Figure 5.23. Examples of pyrite forms at NKM. a) Disseminated pyrite grains from the hangingwall carbonaceous argillite (Sample no. MC01_293). b). Disseminated recrystallised pyrite in carbonaceous argillite (Sample no. MC01_252). c). Strain shadows formed around pyrite grains within carbonaceous argillite (Sample no. MC01_104). d) Zoned pyrite from the southern mine area. The inner core is depleted in Co relative to the outer rim (Sample no. NS002_22m). e). Clean, euhedral pyrite grains surrounded by biotite and calcite (Sample no. MC01_104) f). Pyrite-pyrrhotite grain, fracturing within the pyrrhotite grain (Sample no. MC01_104).

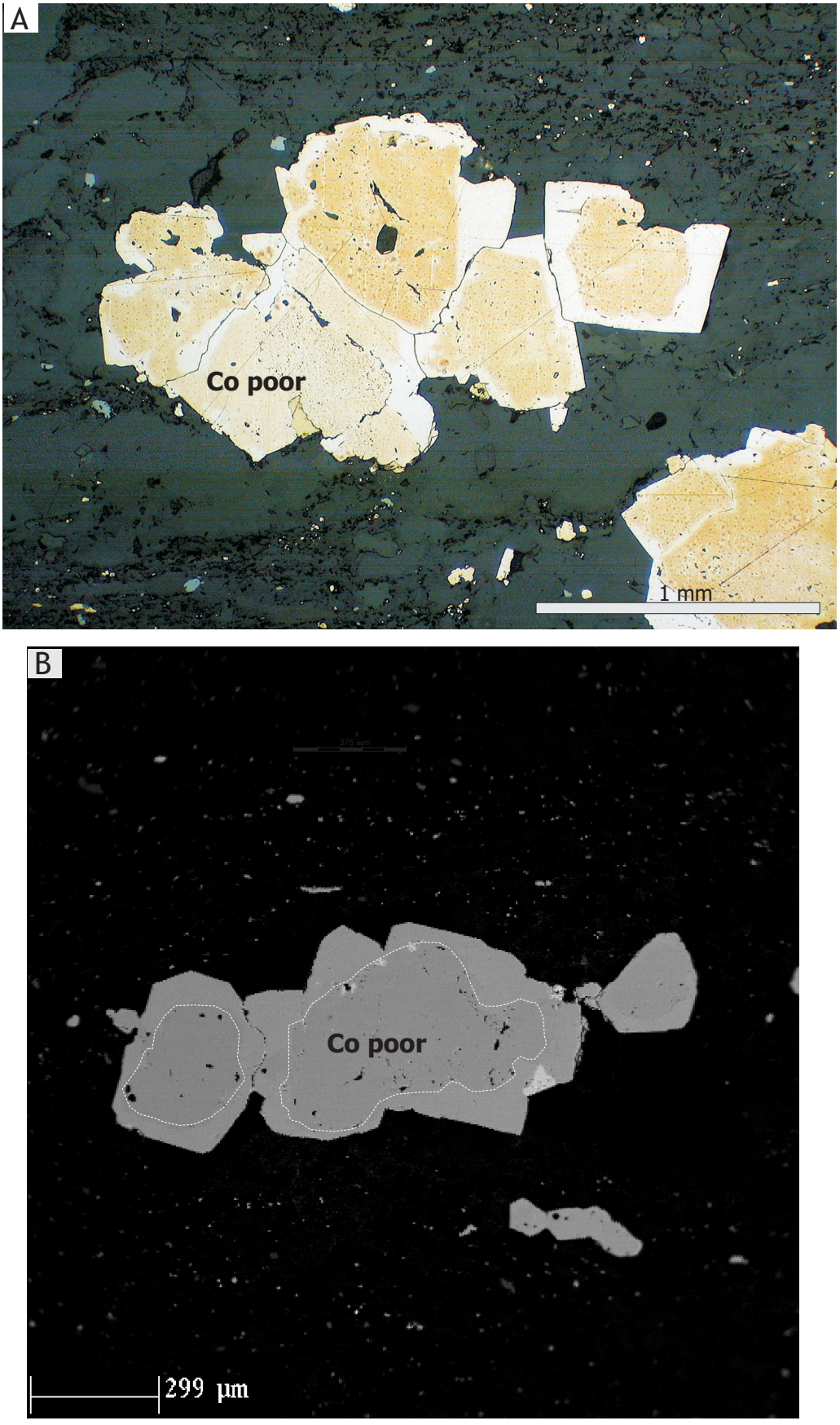

Figure 5.24. Examples of zoned pyrite from drillhole NS015;ca. 299m. a). The inner core has been identified as cobalt poor whilst the outer, inclusion free zone is cobalt enriched. The inner cores commonly have numerous inclusions. b). SEM image shows the inner and outer cores of the pyrite.

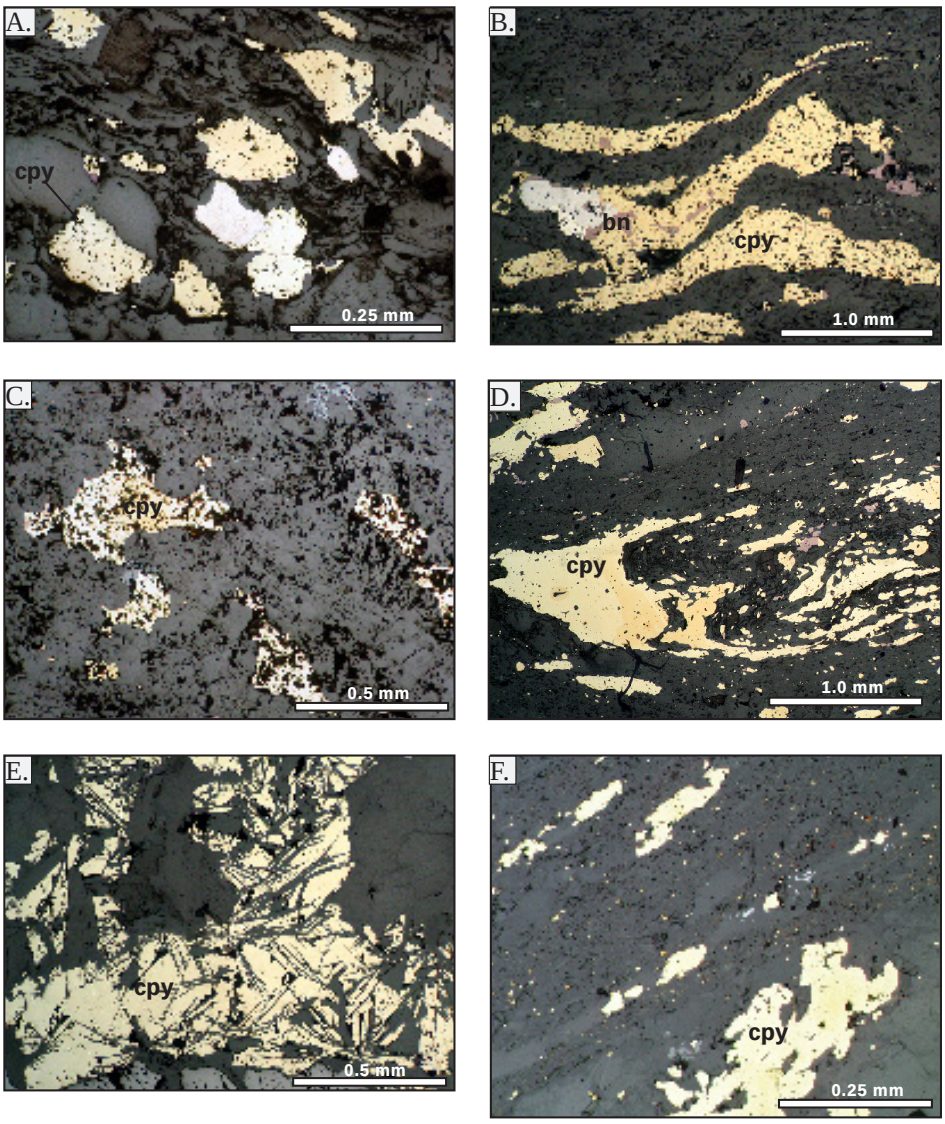

Figure 5.25. a) Chalcopyrite -pyrite hosted within the basal portion of Contact Ore Shale of the COM (Sample No. NS102_12_42m). b). Deformed chalcopyrite-bornite-carrollite (Sample No. NS97_11_no2). c). Inclusion rich Chalcopyrite-carrollite hosted in the COM (Sample No. NS25_41m). d). Deformed chalcopyrite hosted in carbonaceous argillite (Sample no.NS97_4m_5). e). Chalcopyrite overgrown by tremolite and actinolite (Sample NS91_189m). f). Disseminated chalcopyrite and recrystallised aggregates with minor inclusions of silicates (Sample No. NS92_2_13.6m). cpy - chalcopyrite; py - pyrite; bn - bornite; car - carrollite; trem - tremolite.

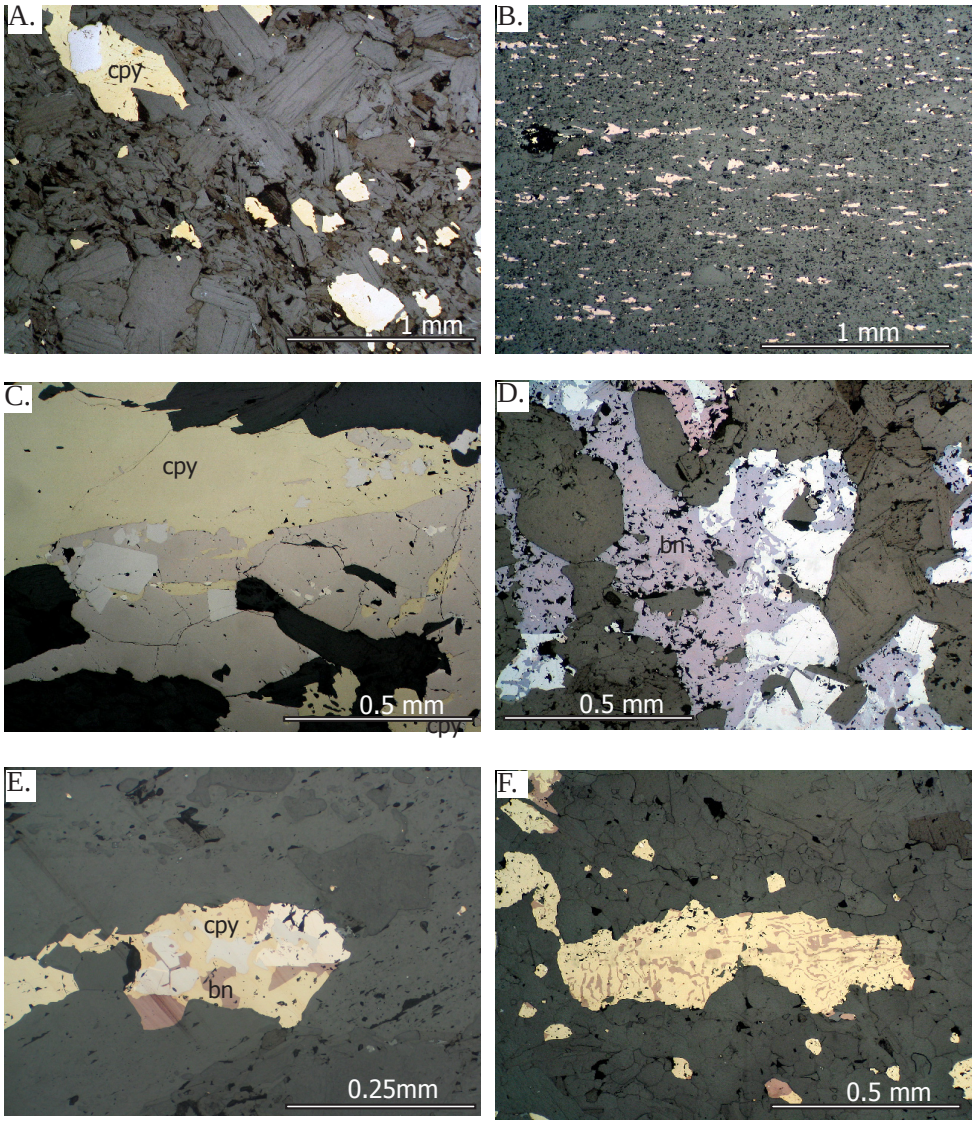

Figure 5.26. a). Carrollite grain overgrown by chalcopyrite (Sample no. NS25_41.1m). b). Disseminated pale purple phase bornite aligned parallel to cleavage (Sample no. NS92_13.6m. c). Chalcopyrite-bornite intergrown, overgrowing pyrite (Sample no. NS97_45.2m). d). Two different phases types of bornite intergrown with late stage carrollite (Sample No. NS92_36.5m). e). Red-orange bornite phase intergrown with chalcopyrite; overgrowing carrollite (Sample no. NS91_61m). f). Exsolution of bornite from chalcopyrite (Sample no. NS92_5.1m). cpy - chalcopyrite; py - pyrite; bn - bornite; car - carrollite; trem - tremolite.

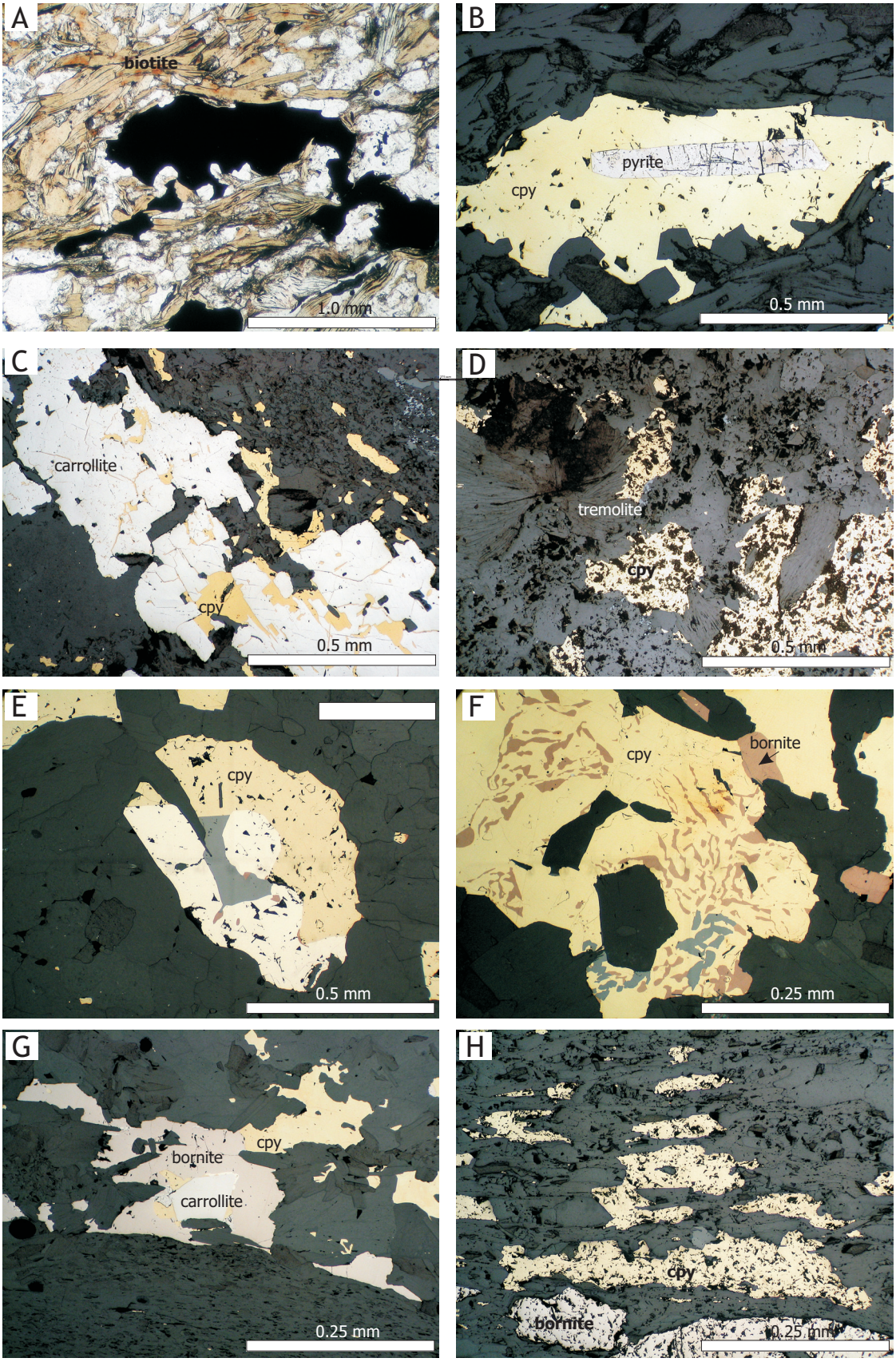

OPPOSITE: Figure 5.27. Examples of sulphide textures within the Contact Ore Shale unit (mine terminology) at the base of the COM within the southern domain. The lithology typically consists of carbonate-quartz-biotite-muscovite-tremolite. a and b). Pyrite enclosed by later stage chalcopyrite with biotite overgrowth (sample no NS025_31.05m). c). Carrollite-chalcopyrite (Sample no NS025_40.1m). d). Chalcopyrite with numerous gangue inclusions (Sample no NS025_41.9m). e). Chalcopyrite-carrollite-bornite (Sample no NS92_2_5_1). f). Chalcopyrite-bornite. g). Carrollite enclosed by bornite-chalcopyrite, no alignment of sulphide to fabric (Sample no. NS97_18_35.9m). h). Inclusion rich bornite and chalcopyrite (Sample no. NS97_18_35.9m). cpy - chalcopyrite; py - pyrite; bn - bornite; car - carrollite; trem - tremolite.

5.7.4 Carrollite Co_2CuS_4 (Cu-rich Linnaeite, Co_3S_4)

Carrollite is light grey to pinkish and occurs as anhedral and subhedral grains that are intergrown with, or overgrown by chalcopyrite and bornite (Figs5.27c and 5.27e). Exsolution lamellae of pyrrhotite are rare and carrollite replaces pyrite. Two phases of carrollite crystallization are identified. The first phase overgrows the earliest pyrite and is light grey and has undergone only minor 'remobilisation' and such carrollite grains may have fractures infilled by chalcopyrite. The second period of carrollite deposition was late- to post chalcopyrite and appears to be one of last sulphide crystallised within the NKM system and may contain inclusions of mica (Figs 5.27c and 5.27g). The later carrollite is associated with some minor occurrences of pentlandite and is confined to the upper portions of the KAM and the Contact Ore Shale. It is common to see fractured carrollite immediately adjacent to recrystallised chalcopyrite and this once again relates to the hardness of carrollite and different metamorphic conditions required to recrystallise the sulphide minerals.

Cobalt predominately occurs associated with carrollite and cobaltiferous pyrite at NKM. Carrollite theoretically should contain 20.5% Cu, however in many of the grains at NKM, the copper contents are less than 20.5%, and are therefore classed as Cu-rich linnaeite. Distinguishing between linnaeite and carrollite is open to debate at NKM and for the purpose of this thesis the term carrollite has been used for linnaeite-carrollite series since it is virtually impossible to identify between the two end-members purely by petrographic observations. Annels and Simmonds (1984) indicate that the thiospinels range from near end member linnaeite (Co_3S_4) to end member carrollite ($CuCo_2S_4$) with the copper content is strongly linked to temperature and sulphur fugacity (Craig et al., 1979). Other cobalt minerals not observed in this study but reported by Annels and Simmonds (1984) include cobaltite, cattierite and cobalt pentlandite.

5.7.5 Accessory Sulphide Minerals

Pyrrhotite $Fe_{1-x}S$

Pyrrhotite is widespread within the carbonaceous argillite hosted copper orebody however was not observed within the mineralised MCF and in the dolomite-argillite lithotypes of the northern domain. Pyrrhotite is commonly found as an accessory mineral in veins, and aligned parallel to, or cross-cutting, the S_2 cleavage. Along the margins of pyrrhotite monoclinic pyrrhotite has been exsolved, and is identified by its higher reflectance and weaker pleochroism compared to the inner core of pyrrhotite. Minor occurrences of exsolved blebs and wisps of pyrrhotite within chalcopyrite grains have been observed.

Sphalerite ZnS

Sphalerite occurs as anhedral grains within the black carbonaceous shales at SOB and is commonly associated with margins of chalcopyrite grains aligned parallel to S_3 cleavage.

Molybendite and Bismuthite

Molybednite occurs as rare 10 to 30 micron subhedral grains. Where present, molybdenite is associated with veins parallel to and cross-cutting the S3 cleavage, and is commonly intergrown with chalcopyrite and bornite. Small 1 cm wide molybdenite only veins were identified within COM on the lower levels at SOB Shaft within the high strain structural domain. Barra et al. (2004) dated molybdenite from cleavage parallel veins at Nkana using Re-Os at 525 ± 3.4 Ma. The absolute age of the mineralising event (s) at NKM will be further discussed in Chapter 7. Other rare phases identified by ZCCM include rickardite (Cu7Te5), tellurobismuthinite (Bi2Te3), veissite (Cu2-xTe) and vulcanite (CuTe).

Gangue minerals

Gangue minerals documented in Chapter 3 and Appendix 1 include k-feldspar, quartz, dolomite/calcite, sericite, albite, tremolite, rutile, graphite and tourmaline (Table 5.5). The recrystallisation and migration of sulphides during metamorphism and deformation was associated with growth of gangue phases such as quartz, calcite, dolomite, albite and phlogopite. These gangue minerals occurred synchronously with the recrystallization of chalcopyrite-bornite.

5.8 DISCUSSION

The meso to micro-scale observations of the ore minerals in relation to lithology and structure is important for determining the timing of mineralisation relative to fabric development. Large-scale remobilisation of sulphide ore will change the ore-host rock relationship and is term external remobilisation. Conversely, internal remobilisation refers to situations where the ore-host rock relationship remains the same however sulphide remobilisation may have taken place within the orebody (Marshall et al., 2000).

The Cu mineralisation, hosted in the lower portion of the COM and the upper portions of the MCF has an overall stratabound geometry in the low and high strain structural domains. . Within the northern part of the orebody, the chalcopyrite-bornite dominated system is associated with facies association COM 1, dolomite-argillite lithotype, while the chalcopyrite-pyrite dominate southern part of the orebody is associated with carbonaceous-carbonate argillite. There are apparent increases in Cu grade coincident with significant changes in the strike of the basement-MCF contact and/or associated with laterally discontinuous facies associations occurring at the base of the COM. Typical the Cu grade appears to decrease away from such zones, adjacent to the Mindola Shaft in the northern part and within the NSA adjacent to the 'C' and 'C-D' anticline-synclines, although deformation has obscured such relationships in part. Strain partitioning and manifestation of syn-orogenic 'fluid focusing' associated with MCF-COM boundary occurred during deformation

The small, though significant, Basal Quartzite Orebody is the only economic, arenite-hosted mineralisation occurring in the lower portions of the MCF at NKM. This orebody is not strictly stratabound, and further contrasts with the stratal geometry of the COM-hosted ores (notably absent in this region) in that it has limited strike length. The Basal Quartzite Orebody is immediately overlain by the laterally restricted carbonate facies (COM 4) of the COM. The orebody is restricted to the most condensed, southern portion of the MCF sub-basin, terminating over a strike length of ~200m with progressive north-westerly thickening of the MCF. The relative timing of the copper mineralisation event in the basal portion of the MCF (Basal Quartzite Orebody) compared to the main copper orebody hosted by the COM is poorly constrained. It was not possible to determine if the copper mineralising events were synchronous, however the folded geometry of the Basal Quartzite Orebody suggest copper mineralising event occurred prior to peak deformation. The same conclusion has been drawn for the main copper orebody at NKM.

Features such as the sulphide bearing veins parallel to foliation and in some cases folded, aggregates of chalcopyrite terminated by foliation and locally fold and the overall morphological and structural features at NKM suggest that primary solid state remobilization did occur and was particularly important on the meso- to micro-scale (Table 5.5). Foliation overprinting and truncation relationships are well preserved in areas at NKM. Growth and/or concentration of cleavage-parallel copper sulphides are timed micro-structurally as syn-D_3. While such relationships may be taken to indicate syn-kinematic metal introduction, the existence of disseminated sulphides in more weakly deformed parts of the orebody that are truncated/overprinted by the S_3 cleavage is considered to provide stronger evidence for modification of a pre-existing sulphide assemblage

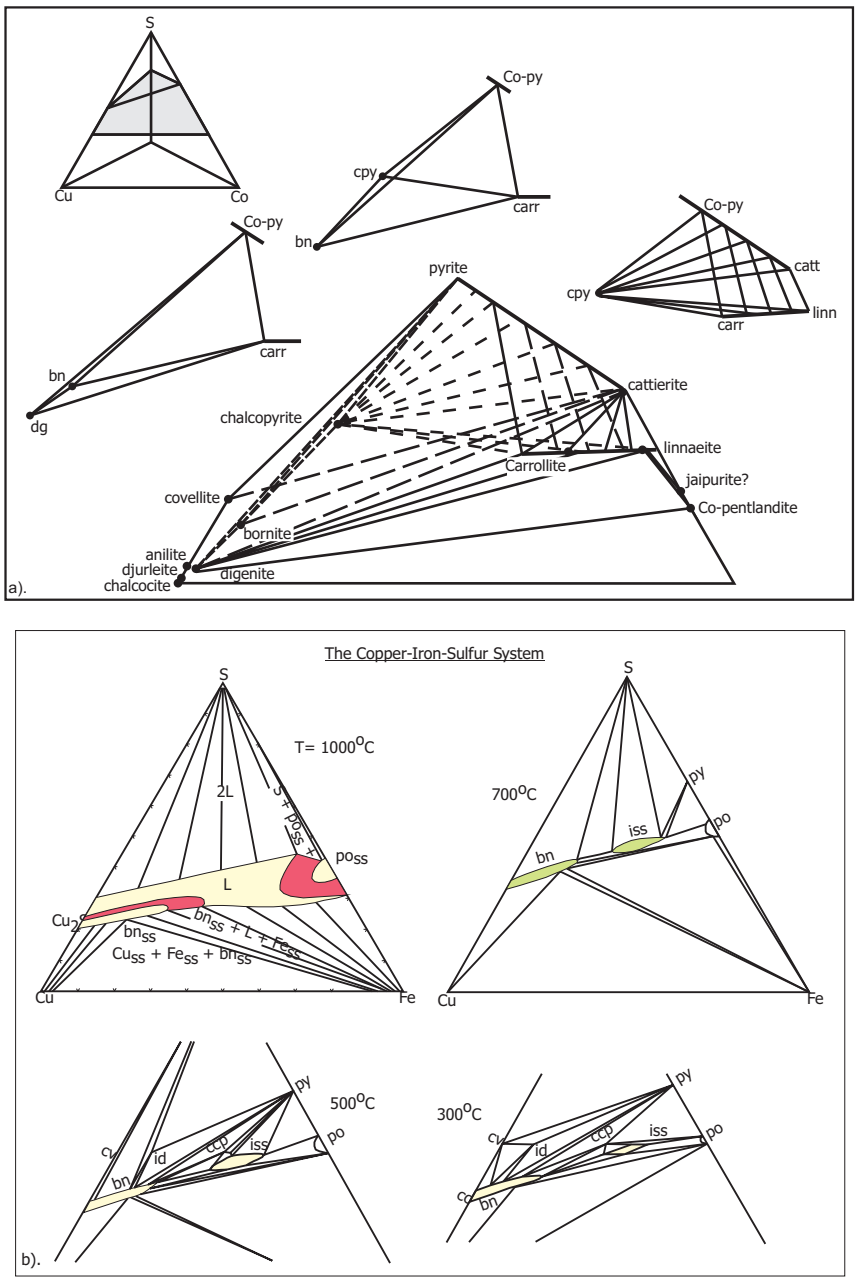

Figure 5.28. a). Phase relations in the Cu-Fe-System at (a) 1000oC, (b) 700oC, c) 500oC and (d) 300oC (adapted from Barton and Skinner, 1979). The phases shown are: L- liquid; bnss- bornite solid solution; iss- intermediate solid solution; py- pyrite; po- pyrrhotite; ccp- chalcopyrite; cv- covellite; id- idaite; cc- chalcocite. b). Low-temperature phase relations in the central portion of the Cu-Co-Fe-S system (from Craig et al., 1979). Craig et al. (1979) document that carrollite typical occur in assemblages with more cobalt-rich pyrites corresponding to decreasing aS2. Therefore inferences can be drawn to the NKM deposit, based on these relationships and the importance of the activity of sulphur in controlling the sulphide assemblage. Some of the more important carrollite containing assemblages are illustrated by the pyramids above the main diagram and are typical of the assemblages at NKM (from Craig et al., 1979).

OPPOSITE: Figure 5.29. a). The brittle-ductile transitions of some common sulphides determined at 5% ductile strain before faulting, and presented as a function of confining pressure against temperature at strain-rates in the order of 7.2 ×10-5 S-1. Lines A, B and C represent geothermal gradients of 200, 350 and 600C km-1, respectively, for a geobaric gradient of 25 MPa km-1(from Marshall and Gilligan, 1987). The much greater strength of pyrite is responsible for its much more refractory behaviour during metamorphism and this is clearly observed at NKM as bornite and chalcopyrite clearly shows evidence of deformation while pyrite does not exhibit such characteristics. b). Simplified log aS2-1 vs. Tplot showing the pyrite-pyrrhotite sulphidation curve which buffers the activity during the metamorphism of pyrite-pyrrhotite ores (from Barton and Skinner, 1979). Pyrite-pyrrhotite occur only within the high strain domains at NKM and exhibit textural relationships suggesting pyrrhotite growth. c). Two schematic diagrams of Fe-S systems documenting pyrite and/or pyrrhotite growth or corrosion during increasing and decreasing temperature (from Craig and Vokes, 1993). The association of pyrite and pyrrhotite only occurs within the high strain structural domain at NKM clearly demonstrates metamorphic recrystallisation of the majority of sulphide assemblages.

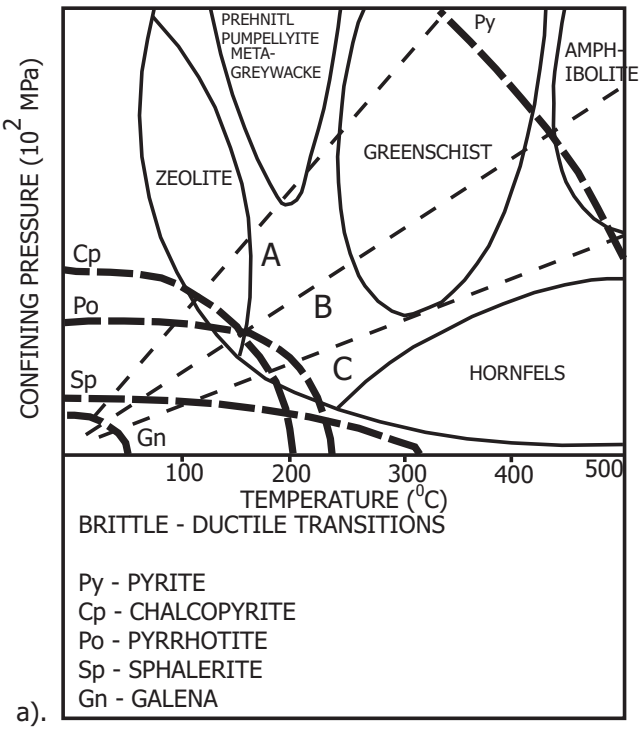
PREHNITL
PUMPELLYITE
META-
GREYWACKE
Py
AMPH-
IBOLITE
ZEOLITE
GREENSCHIST
Cp
A
Po
B
C
Sp
HORNFELS
Gn
CONFINING PRESSURE (10^2 MPa)
100
200
300
400
500
TEMPERATURE (°C)
BRITTLE - DUCTILE TRANSITIONS
Py - PYRITE
Cp - CHALCOPYRITE
Po - PYRRHOTITE
Sp - SPHALERITE
Gn - GALENA

a).

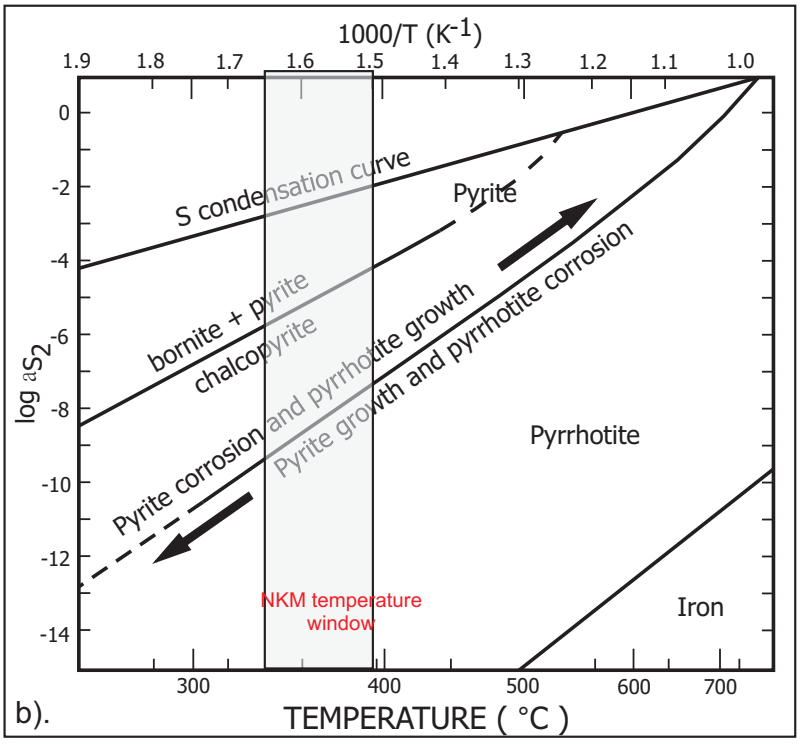
1000/T (K-1)
1.9
1.8
1.7
1.6
1.5
1.4
1.3
1.2
1.1
1.0
0
-2
-4
-6
-8
-10
-12
-14
log aS2
S condensation curve
Pyrite
bornite + pyrite
chalcopyrite
Pyrite corrosion and pyrrhotite growth
Pyrite growth and pyrrhotite corrosion
Pyrrhotite
NKM temperature window
Iron
300
400
500
600
700
TEMPERATURE (°C)

b).

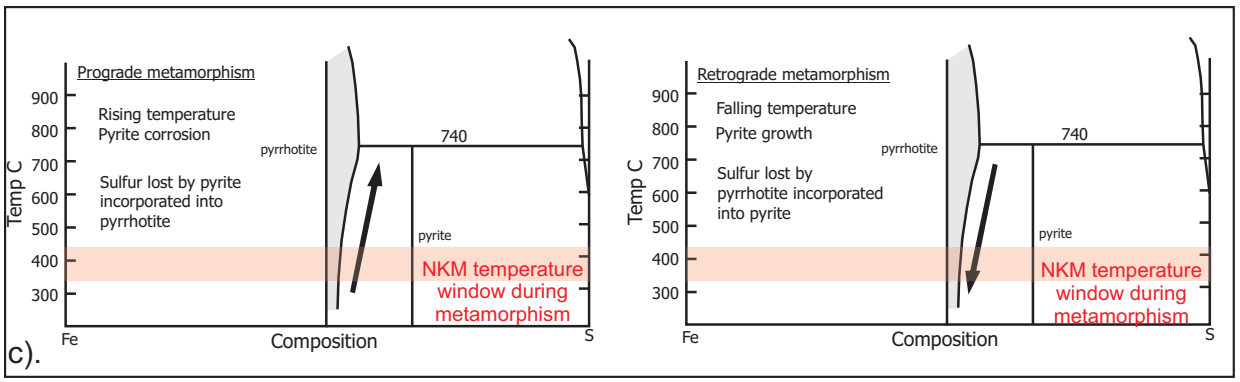
Prograde metamorphism
Rising temperature
Pyrite corrosion
Sulfur lost by pyrite incorporated into pyrrhotite
pyrrhotite
740
pyrite
NKM temperature window during metamorphism
Temp C
900
800
700
600
500
400
300
Fe
Composition
S
Retrograde metamorphism
Falling temperature
Pyrite growth
Sulfur lost by pyrrhotite incorporated into pyrite
pyrrhotite
740
pyrite
NKM temperature window during metamorphism
Temp C
900
800
700
600
500
400
300
Fe
Composition
S

c).

during deformation. Given that paragenetic relationships between various sulphide phases are similar in low- and high-strain environments (except for localised late-stage carrollite growth) recrystallisation of the mechanically weak Cu-sulphides is considered to have involved largely grain-scale modification of pre-orogeneic orebody configuration. Supporting this interpretation is the preservation of stratabound orebody geometries in all parts of the system, regardless of the intensity of strain. The effects of upper greenschist facies metamorphism and deformation at NKM are interpreted to have led to variability recrystallised sulphide textures.

The extent to which recrystallisation has occurred was governed by the mobility of the individual mineral species and the form in which they were transported during metamorphism. Table 5.5 summaries the paragenetic sequence of sulphide growth at NKM, based on the following relationships:

- The earliest pyrite phase is interpreted to be late diagenetic origin and typically replaces an earlier diagenetic phase of anhydrite and/or dolomite (e.g. Annels, 1989). The timing of the earliest phase relative to deformation is indicated by the rotation of some pyrite grains occurs in high strain domains suggesting pre-kinematic. At the weakly deformed Chambishi SE prospect, black carbonaceous argillite host pyrite grains with 'spongy' looking cores which have the isotopically lightest S signature and can be interpreted as typical of early diagenetic Fe sulfides based on similarities seen in other sedimentary rocks (e.g. Raiswell and Berner, 1986). No similar pyrites were identified within the carbonaceous-carbonate lithotype at NKM as recrystallization of these pyrite grains occurred in the high strain domains during peak metamorphism. Later generations of pyrite or pyrite recrystallization (pyrite 3) are synchronous or post-dating peak deformation.
- Chalcopyrite, bornite, carrollite, and pyrite are the main sulphides. One phase of chalcopyrite and carrollite overgrows and/or replaces pyrite. A second generation of chalcopyrite-bornite frequently overgrows carrollite, or encloses fractured carrollite. A volumetrically minor late stage of carrollite, confined to the high strain domain, overgrows both chalcopyrite and bornite. Chalcopyrite and bornite have been recrystallised and locally remobilised during peak deformation and metamorphism and are commonly aligned parallel to S_3 cleavage and intergrown with, or overprinted by, silicate minerals.
- Phlogopite, K-feldspar, dolomite/calcite and sericite are the dominant gangue mineral phases in the mineralised horizon, with minor tourmaline, rutile, and apatite.
- All mineralised veins are confined to the stratabound, folded copper orebody envelope and regardless of their generation, contain a similar sulphide and gangue assemblage to the host lithology.

5.8.1 Sulphide Stability during Metamorphism

Deformation and metamorphism has resulted in the localised deformation and remobilisation of the sulphides on the scale of centimetres to metres within the confines of the stratabound copper ore envelope. The mechanical remobilisation of sulphides requires a rheological contrast between that of the sulphide and the host rock (Marshall and Gilligan, 1987). Sulphides can be ranked according to strengths from weakest to strongest; galena<pyrrhotite<chalcopyrite<sphalerite<pyrite. The addition of an aqueous phase will further modify the mechanical behaviour, in such a way that intercalated sulphides and silicates undergo a complex interplay of solution transfer and other mechanisms (Marshall and Gilligan, 1987). Gilligan and Marshall (1987), Boyle (1993) and Craig and Vaughan (1993) have examined the complex textural responses of chalcopyrite, bornite and chalcocite to temperature changes (Figs 5.28a and 5.28b). It is estimated that temperatures during metamorphism at NKM were in excess of 400°C, therefore the complex intergrowth textural relationships between bornite-chalcopyrite-carrollite are the result of recrystallization during metamorphism. The metamorphic mobilisation, as defined by Marshall and Gilligan (1993), occurring on a micro- to meso-scale is an important process resulting in the increased concentration of sulphide at favourable sites either by chemical

Table 5.5. Relative interpreted timing of the sulphide and gangue assemblages at NKM. Upper greenschist facies metamorphism has resulted in the sulphides hosted in MCF and COM being recrystallised, therefore the textural relationships, particularly of the copper sulphides, are metamorphic, however by combining the textural information with the orebody geometry further inferences can drawn regarding the original paragenetic sequence.

Mineralogy	**Pre-Tectonic** (pre/syn-D2)	**Syn-tectonic** (syn-D3/remoblised)	**Late-tectonic** (post-D3/remobilised)	**Supergene / Weathering**
Disseminated Sulphides hosted by COM and MCF				
Pyrite				
Co pyrite				
Chalcopyrite				
Bornite				
Pyrrhotite				
Carrolite				
Molybendite				
Bismuthite				
Gangue Mineralogy of COM and MCF				
Quartz				
Dolomite/Calcite				
Muscovite-Sericite				
Phlogopite				
Albite				
Tremolite- Actinolite				
Talc				
K-fledspar				
Anhydrite				
Vein hosted Sulphides (veins confined to stratabound orebody geometry)				
Pyrite	VI	VII	VIII	
Co pyrite				
Chalcopyrite				
Bornite				
Pyrrhotite				
Carrolite				
Molybendite				
Bismuthite				
Secondary Copper minerals				
Malachite				
Chrysocolla				
Curite				
Azurite				
Tenorite				
Libethenite				
Chalcocite				
Covellite				
Native copper				

Table 5.6. Summary table of the criteria and important observations made during this study to distinguish between the pre-tectonic and syn-tectonic mineralising events (original table format modified from Marshall and Spry, 2000).

Guideline	Observations	Interpretation
Preservation of primary textures in sulphides and altered host rocks	Very dissemination grains and 'spongy' looking grains at Chambishi SE (McGoldrick and Cooke, 2003)	Pre-tectonic
Map-scale relationship between ore zonation, alteration and primary layering	Stratiform to stratabound copper ore geometry concordant with primary host-rock layering. Pre-deformation geometry of orebody known from undeformed deposits (Selley et al., 2005) and systematic relationship between the ore and host. Regional scale alteration documented by Selley et al. (2005). Localised alteration confined to basal ore zone/ high strain domains. Orebody conforms to folded stratigraphy.	Pre-tectonic or early syn-tectonic
Foliation overprinting relationships	Sulphides parallel to S_2 cleavage and stratiform sulphides locally folded about micro- and mesoscale F_3 closures. Strain shadows developed around pyrite grains. Sulphides overprinted by retrograde metamorphic mineral.	Pre-tectonic and/or syn-tectonic
Foliation truncation relationships	Truncation of primary layering by S_3 parallel veins hosting sulphide. S_3 foliation overprints bedding parallel veins	Syn-tectonic or pre-tectonic
Strain distribution in ore, altered and unaltered host rocks	Higher strain in the less competent lithotypes of the COM. No contrast in strain between unmineralised and mineralized host rocks.	Remobilised syntectonic origins / remobilized pre-tectonic ore
Distribution of full and partial structural history in ore and host	Textures and structural alignment associated with chalcopyrite and bornite indicate remobilisation during deformation. Host sequence and orebody have undergone the same deformation.	Pre-tectonic
Metamorphic assemblage relationship to ore and host	Metamorphic assemblage in host rock overprint and/or intergrown with sulphides; sulphides in high strain domain aligned parallel to cleavage and locally cross cutting cleavage	Syn-tectonic or pre-tectonic
Porphyroblast/matrix relationships	Quartz-calcite-mica formed in pressure fringes of rotated pyrite grains	Pre-tectonic

(solution, diffusion, volatile transport), transitional (partial melting) or physical (plastic flow) processes. In addition to this, given the variation in strain across the NKM deposit and changes in the deviatoric stress between different sites would have also influenced the distribution of the sulphides.

Pyrite is commonly stable in the greenschist to amphibolite grades as long as the activity of sulphur remains high (Craig and Vokes, 1993) (Figs 5.29a and 5.29b). However recrystallisation of pyrite at greenschist facies and above will regularly lead to the development of annealed textures and changes in grain size (Craig and Vokes, 1983). Furthermore Cox (1987) and Cox et al (1981) documents the hardening of pyrite during plastic deformation. Pyrite, unlike many of the copper sulphides has significantly more strength in terms of differential stress and temperature due to its bond strength and commonly forms idiomorphic cubic crystals during prograde and retrograde metamorphism at greenschist facies and higher, since it has the tendency to recrystallise thus influencing grain size and appearing as annealed textures (Craig and Vokes, 1993). Pyrite at NKM commonly has a cubic form, exhibits rare preferential elongation alignment to S_3 cleavage unlike chalcopyrite and bornite, which are commonly observed aligned parallel to cleavage in high strain areas and euhedral pyrite grains may have strain shadows developed of mica. These observations tend to suggest that a large proportion of pyrite was stable during deformation or that growth took place during peak or post-peak metamorphic periods. The observations of pyrite-pyrrhotite intergrowths and corroded pyrite supports high temperatures (~400^{o}C) during metamorphism as the decomposition of pyrite to pyrrhotite occurs in the 300 to 600^{o} degree range during prograde metamorphism (Craig and Vokes, 1993). The degree to which decomposition occurs during prograde metamorphism is also a function of an increase in the activity of sulphur while conversely a decrease in sulphur activity occurs during retrograde cooling resulting in the growth of pyrite (Craig and Vokes, 1993) (Fig. 5.29c). Therefore, the association of pyrite-pyrrhotite at NKM is interpreted to be a function of temperature and the variation in sulphur content during prograde and retrograde metamorphism.

5.9 SUMMARY

- The copper mineralisation at NKM is hosted by the Lower Roan Group, within the upper portion of the MCF and predominantly within the basal portion of the COM.
- The copper orebody has a stratabound geometry and was deformed during the main deformation phase (herein defined as D_3).
- There is recognisable lateral zonation of copper sulphides across the NKM, with a bornite-chalcopyrite dominant assemblage in the north and a chalcopyrite-pyrite assemblage in the south. The change in sulphide assemblage is coincident with a change from the northern dolomite-argillite facies association to the carbonaceous-carbonate facies association in the southern part.
- Vertical zonation is variable; however there is a recognisable uniform pyritic hangingwall to the copper orebody across both the northern and southern domains and occurs in the same laterally extensive facies association.
- There is an increase in the copper grade at three localities coincident with changes in the basement-MCF geometry and local facies within the lower COM. These locations were interpreted from sedimentological and structural information as evidence of inherited basin structures. The apparent association of broad variations in the copper distribution, coincident with these locations, suggests that the original basin geometry and facies did influence the migration of fluids through the permeable MCF and along basin faults, the availability of sulphur (anhydrite +- pyrite) from the different facies associations of the COM and by providing a chemical and/or facies-structural trapping mechanism. This conclusion is supported by studies at the weakly deformed Chambishi SE and Mwambishi B deposits which document a clear relationship between copper distribution and basin geometry at weakly deformed deposits.
- Sulphide remobilisation occurred during deformation/metamorphism resulting in the localised concentration of sulphides aligned parallel to cleavage, in fold hinges and in syn-tectonic veins within the high strain structural domain. Cobalt is irregularly distributed within the copper ore envelope and there appears no systematic relationship to lithology and/or structures. The cobalt distribution within the ore deposit is complex and there is a variation in the Cu/Co ratios about fold hinges interpreted to be relating to the varying mobilities of the copper and cobalt and to the variations in structural induced permeability during the precipitation of the sulphide phases as part of the syn-tectonic mineralisation event/remobilisation.
- The fine grained disseminated pyrite hosted within the COM is considered to be diagenetic origin, however the exact timing is unknown. Late stage syn-tectonic pyrite and vein hosted pyrite does occur predominately confined within the copper ore envelope. There is internal zonation of some pyrites, with an outer rim exhibiting enrichment in cobalt. The lack of evidence of large quantities of early pyrite could be a function of remobilisation or more likely resulting from the pyrite being consumed by copper and thus acting as an in situ source of sulphur, particularly in the carbonaceous-carbonate argillite facies.
- The main phase of copper mineralisation is pre-tectonic (pre-D_3) based on several lines of evidence including the overall folded orebody geometry, the remobilisation of sulphides into alignment with S_3 cleavage and the internal deformation of sulphides. Textural evidence suggests deformation resulted in the remobilisation of copper sulphides in a dynamic and progressive manner particularly within high strain structural domains. The layer ductility contrasts between adjacent horizons has played a role in the determining the amount of sulphide remobilisation during deformation/metamorphism as is observed when comparing textures of sulphides hosted in the fine- and coarse-grained beds within the COM.
- The recognition of Co-enriched phases of pyrite particularly in the southern facies association and significant quantities of carrollite in both facies associations suggests cobalt was closely associated with the Cu

mineralising fluid and the precipitation (or remobilisation) of the sulphide was a function of changing activity of sulphur at a meso-scale during mineralising events.

- The different vein generations hosting sulphides are confined within the overall folded copper ore envelope. There are limited observations of sulphide hosting veins beyond the main copper ore envelope, suggesting the main source of the sulphide for veins was from immediate host rock.
- Leaching of the ore minerals has taken place during supergene processes with malachite common along fractures near surface.

The northern and southern copper orebodies are hosted in the upper portion of the MCF and basal zone of the COM. The semi-continuous and transgressive character of the orebody across the MCF-COM stratigraphic boundary, the folded orebody geometry and the observed textures suggest that the majority of copper sulphides pre-dated the development of S_3 cleavage. Peak metamorphism resulted in localised sulphide remobilisation and the development of ambiguous textural relationships for the ductile sulphides and recrystallised of gangue mineralogy thereby obscuring early textural relationships. By documenting the copper orebody geometry and relationship to stratigraphic sequence in low and high strain domains at NKM, it can be adequately concluded internal remobilisation of sulphides took place during orogenesis and a syn-orogenic mineralising event did occur.